Title

Structural Behavior of Tubular Joints With Wing Plates

Author

Bouwkamp, Jack

Publication Date

1967-11-01

REPORT NO.
67-32

STRUCTURES AND MATERIALS RESEARCH
DEPARTMENT OF CIVIL ENGINEERING

STRUCTURAL BEHAVIOR OF TUBULAR JOINTS WITH WING-PLATES

BY

J. G. BOUWKAMP

Report to the Sponsor: Kaiser Steel Corporation, Fabrication Division

DECEMBER 1967

STRUCTURAL ENGINEERING LABORATORY
COLLEGE OF ENGINEERING
UNIVERSITY OF CALIFORNIA
BERKELEY CALIFORNIA

Structures and Materials Research
Department of Civil Engineering
Division of Structural Engineering
and Structural Mechanics

BEHAVIOR OF TUBULAR JOINTS WITH WING-PLATES

A Report of an Investigation

by

J. G. Bouwkamp
Professor of Civil Engineering

to

Kaiser Steel Corporation
Fabrication Division
Oakland, California

College of Engineering
Office of Research Services
University of California
Berkeley, California

December 1967

TABLE OF CONTENTS

LIST OF FIGURES

Number

LIST OF FIGURES
(Continued)

STRUCTURAL BEHAVIOR
OF TUBULAR JOINTS
WITH WING-PLATES

I. INTRODUCTION

I-1. General

Offshore drilling structures in shallow waters are generally designed as multi-legged towers. The column members in these eight- and twelve-legged structures normally vary from 3 to 4 feet in diameter. The truss web members in such instances are about 18 inches in diameter and are welded to the column members after being profiled and beveled to fit the column sections.

Recent developments in the design of stationary and mobile platforms for deep ocean exploration have resulted in trussed offshore structures with only three, four and six column legs. The same trend has been observed in the design of truss-type production platforms for waters with heavy ice flow, like Cook Inlet, off the coast of Alaska. The diameter of the column members in such structures often ranges between 12 and 20 feet, while the branch members vary between 6 and 8 feet.

The load transfer in the traditional multi-legged towers is achieved almost exclusively through a direct connection of the joining members. Earlier studies have indicated that a joint with non-overlapping branch members and a column-wall thickness of 0.05 O.D., in which

O.D. is the outer diameter of the column member, has a superior fatigue life as compared to joints with overlapping branch members or gusset plates [1] [2]. However, for large diameter column members, a column-wall thickness requirement of 0.05 O.D. becomes economically and even practically unfeasible. Therefore, other design concepts, although possibly resulting in joints exhibiting a reduced fatigue life, have to be adopted. Firstly, by using in-plane gusset plates, a large fraction of the member forces can be transferred into the gusset plate, thus reducing the direct web member forces on the column member wall. Secondly, by employing large curved back-up plates inside the column members, the load transfer from the web members to the column member will be distributed effectively. In most designs, a combination of these two concepts is encountered. For instance, a cement-grout filled column member with internal diaphragms or ring stiffeners, to provide a back-up for the column wall, together with either external wing-gusset plates or flared-out web member sections, to increase the contact perimeter between the web members and the column member, is a typical example of an integration of these basic design concepts.

---

[1] Bouwkamp, J. G., Tubular Joints Under Static and Alternating Loads, Report No. 66-15, June 1966, Structures and Materials Research, Department of Civil Engineering, University of California, Berkeley.

[2] Bouwkamp, J. G., Considerations in the Design of Large-Size Welded Tubular Truss Joints, Engineering Journal, AISC, vol. 2, No. 3, July 1965.

I-2. Objective and Scope

The objective of this study was to evaluate the effectiveness of wing-plates or external gusset plates in a large-size tubular joint under both static and alternating loads. This type of design has been used for platforms located in Cook Inlet, Alaska. Such structures have four large-diameter column legs and a single cross-braced panel in each vertical, external truss plane. Figures 1 and 2 show a 1:7 scale model of an actual joint as studied in this investigation. The column section has an inner and outer wall with a cement-grout fill between those two sections. This fill provides the radial stiffness for the thin - 0.01 O.D. - column wall. The objective was to study the joint strength with and without the triangular external wing-plates.

A total of six specimens were fabricated, three with and three without wing-plates. The wing-plates were only used between the diagonal and the column member because the load transfer between the horizontal web member and the column was insignificant.

A sample of both types of joints was instrumented substantially with electrical resistance strain gages to study under static loads the stress distribution and load transfer in these joints under both compression and tension in the diagonal. The strain gages, with a grid length of 1/4 inch, were either single, cross, or rosette gages, and were, when applicable, invariably placed as close as possible to the weld. In addition to the strain gages placed in the direct vicinity of the joint, a number of cross gages were applied to evaluate the efficiency of the composite column member under bending. This instrumentation was radially distributed in a horizontal section on the outside of the column member of the non-wing-plate model joint.

The initial two specimens were tested until failure under static loads occurred. Two of the four remaining specimens were tested unaltered under alternating fatigue loads. The final two specimens were tested both under static and alternating loads. These last two joints were modified versions of the original wing-plate type joint.

I-3. Acknowledgments

It is gratefully acknowledged that the studies reported herein were sponsored by the Fabrication Division of the Kaiser Steel Corporation through a grant to the Graduate Division, University of California, Berkeley. The project was carried out under the direction of Professor J. G. Bouwkamp, Division of Structural Engineering and Structural Mechanics, Department of Civil Engineering. The experimental phase of the project was performed at the Structural Research Laboratory of the Division of Structural Engineering and Structural Mechanics, Richmond Field Station, Richmond, California.

The author wishes to acknowledge Mr. A. J. Tokola, Manager, Construction Engineering, Fabrication Division, Kaiser Steel Corporation, for his cooperation in achieving an early completion of the testing phase of the program.

Also, the invaluable assistance of Messrs. J. Bradford, Assistant Development Engineer, O. Greste, Junior Specialist, and A. Makrinassios and H. Papageorge, Engineering Aids, is hereby gratefully acknowledged.

II. TEST PROGRAM

II-1. General

The initial objective of this program was to perform a comparative study of a joint with and without wing-plates under both static and alternating loads. However, through an extensive instrumentation of the two basic joints, significant information to further improve the wing-plate joint could be obtained. The instrumentation was therefore designed to give information regarding the general load transfer in these joints and the state of stress in presumably critically stressed areas of both the diagonal and column-tube walls. Due to an expected limited non-linearity of the composite tube section, a different behavior of the joints under large completely reversed loads was anticipated. Therefore, the static load studies were carried out for both compressive and tensile forces in the diagonal members. Strain gages were recorded for step-wise increased static loads only.

The fatigue studies were carried out under fully alternating loads simulating critical design conditions.

The joint configuration tested represents a typical upper joint of a single cross-braced panel. This panel is entirely submerged under normal conditions, so that only the upper part of the column legs and the platform appear above the water. The diagonal member force at this upper nodal point is most severe.

II-2. Joints

The wing-plate test joint is a 1:7 scale model of an actual truss joint with a 14-foot diameter column member. The test joint has a horizontal web member and a diagonal member which make an angle of approximately 55° with the column section. Figures 1 and 2 show the detailed dimensions of the member sections for the wing-plate joint. The other joint, without wing-plates, is identical to the one shown in the figures except for the absence of these plates. The steel used in these joints is ASTM A 441 except for the horizontal member which is fabricated of ASTM A 36 steel. The load P applied to the load-application point as shown in Figure 1, represents the effect of the alternating forces due to wind, waves and ice flow acting on the tower. While these loads produce very large forces in the diagonals of the cross-braced panel, the effect of these external loads on the horizontal member can practically be neglected. Consequently, wing-plates have only been designed for the diagonal-to-column connections. To carry out this study three identical specimens of each of the two joint types were fabricated.

As will be discussed in detail in Chapter III, comparative results for the two types of joints under both static and alternating loads clearly established the superior performance characteristics of the wing-plated joint design. These conclusions were derived after testing two specimens of each type, one under static loads up to failure and one under full alternating loads until failure was initiated.

The remaining two specimens were used in an attempt to improve further the wing-plated joint design, to the extent that the third wing-plate specimen was modified as shown in Figure 3, by an in-plane extension of each wing-plate with a triangular plate to fill the corner between the wall of the diagonal and the original 90° cut-off edge of the wing-plate. This arrangement would result in the necessary reduction of the stiffness step between the flexible 1/16-inch thick tube wall and the wing-plate with its relatively large rigidity in its own plane.

An additional modification shown in Figure 3 was the welding of a 1/8 x 1 inch stiffener strip to the outside of each wing-plate in order to increase the buckling strength of this plate. These strips were welded on top of the upper and underneath the lower wing-plates.

The above modified wing-plate design was first studied under a limited static load in order to evaluate the load transfer from diagonal to column member. Next, the joint was subjected to an alternating fatigue load until failure occurred.

Based upon the above results, it was decided to redesign the wing-plate and to incorporate and test this new design in the last specimen (which originally had no wing-plates). Figure 4 shows the revised wing-plate design. It should be noted that the thickness of the upper wing-plate, on the side of the horizontal member, is 3/16 inch. The thickness of the lower wing-plate is unchanged and is 1/8 inch. The material used was specified to meet the minimum requirements of ASTM A 441.

II-3. Instrumentation

The initial electric-resistance strain gage instrumentation for the two basic joints was designed to evaluate the stress levels at several presumably critical locations. Therefore, the wing-plate specimen was instrumented with 23 rosette, 10 cross and 7 single gages, thus resulting in 96 separate gage grids. All gages used in these studies were of the Shinko type with a gage length of 1/4 inch. The gages were placed almost exclusively on the walls of the diagonal and column members near the welds between the wing-plates and these tube sections. Figures to be presented in Chapter III, and showing the principal stresses and directions, give a more specific indication of the strain gage location and distribution. The strain gage instrumentation for the non-wing-plate joint was designed to provide information regarding the state of stress in the tube walls near the welds between the diagonal and column section. In addition, a number of cross gages were placed along a 200° arc of a normal section of the column tube to evaluate the bending effectiveness of the composite column member. Again, more specific information regarding the location of the 96 gage circuits (13 rosette and 28 cross gages and 1 single gage) is given in Chapter III.

After the results of the above initial studies showed a very efficient performance of the wing-plate joint, the subsequent investigation was directed towards a further improvement of the wing-plate design. This was carried out in several steps. First, the two wing-plates on one side of the modified wing-plate joint were instrumented with photo stress on one side of each plate to evaluate the principal stress direction in these plates in general, but particularly along the throat section A-A — see Figure 3. The expectation that the principal stress direction in gusset plates with an approximate 1:2 taper is parallel to the free edges, as based on results from earlier studies on photo elastic models of tubular gusset plate joints, was found to be also correct in this case. It was realized that the effect of the one-sided surface stresses, as observed, did not necessarily represent the true in-plane stress transfer in these plates. However, the principal stress directions recorded along the throat sections were considered predominantly a result of in-plane forces and not of bending moments. Therefore, the subsequent cross gage instrumentation along the throat sections to evaluate the total force transfer through these wing-plates was oriented parallel and normal to the free edge of these wing-plates. Two wing-plates on one side of the truss plane were instrumented with 20 crosses and 4 singles. These gages were all arranged in a back-to-back fashion to allow the separation of strains caused by in-plane forces and bending moments. An additional 4 cross gages were placed on the wing-plates located on the far side of the truss plane in order to check the load symmetry with respect to the plane of the truss. The resulting 52 strain-gage grids were recorded on a fully automatic Gilmore strain recorder with a simultaneous plotting and printing output. This unit has been used for all static strain recording purposes.

The final strain gage studies dealt with evaluating the load transfer through the wing-plates of the revised joint design shown in

Figure 4. For this purpose, the two wing-plates on one side of the truss plane, as well as the wall of the diagonal tube on that same side, were instrumented with 12 rosette and 52 cross gages, for a total of 140 strain gage circuits. Fourteen cross gages were placed back-to-back along the throat section of the two wing-plates. The 12 rosette gages were located near the welds between these wing-plates and the column wall. The remaining cross gages were placed in 5 cross sections located along the wall of the diagonal tube and spaced at intervals of 2.5 and 3 inches. Each section incorporated 5 to 7 cross gages, which were invariably placed along the axial lines of symmetry and along longitudinal sections close to either side of the welds between the wing-plates and the diagonal tube wall. To check load symmetry, an additional set of 4 cross gages was placed in a normal section of the diagonal at 90° intervals coinciding with the axial lines of joint symmetry (formed through intersection of the diagonal tube wall with two orthogonal planes, one of which is the truss plane).

II-4. Loading

Under the design-load conditions, the diagonal member acts as the strut or tie in order to react the lateral loads acting on the tower structure. These loads introduce a considerable moment in the column section above the upper cross-bracing joint under study. At the same time, the horizontal web member carries practically no load at all. To realize these loads in the model, a special loading frame, as shown in Figure 5, was designed and fabricated by the sponsor. The joint specimen was mounted in this frame by pin connections at both the base of the column member and the diagonal. Since the horizontal member was insignificant in the load transfer, the end of this member was kept entirely free from the frame. The load applied to this system was provided by a double acting hydraulic load cylinder with a maximum dynamic capacity of + and -80k. The static load capacity is ± 120k.

Considering the diagonal member and the composite column section with a moduli ratio E_{st}/E_g of 7.5, the reaction forces for this statically indetermined system have been calculated. The force diagram in Figure 5 shows the resulting reactions. It should be noted that for an applied load of 50k the reaction force of 113k in the diagonal is, for all practical purposes, an axial load. Only a very small eccentricity exists and results in a moment of only 5 k in at the joint. The nominal stresses at the joint resulting from the axial load and moment are 30.4 ksi and ± 1.3 ksi, respectively. If the steel in the column section is assumed to act as an integral section, but the grout is neglected entirely, the above results remain practically unchanged.

III. EXPERIMENTAL RESULTS

III-1. General

The results of the experimental studies are presented in two sections. Although in the actual investigation the static and alternating load tests were not carried out in separate order, the results are nevertheless presented in a grouped fashion. Considering the urgent need for information at an early stage concerning the ultimate strength under static loads of the two basic joints, the wing-plate joint was tested first, followed by the non-wing-plate joint. During these static load studies the loads were increased step-wise in alternating fashion. Because of the expected larger strength of the joint under a compressive load in the diagonal, a compressive load was invariably applied first, followed by a zero load and subsequently a tensile load of the same magnitude as the earlier compressive load. Then, after reducing the load to zero, a higher compressive load was applied to the specimen and the loading procedure was repeated until failure occurred. The experimental results from these two tests are presented first, followed by the results of the static load studies carried out on the modified joint, shown in Figure 3. This joint was subjected to static cylinder loads of + and -60k, and was not brought to failure under static loads. The same joint was then subjected to fully alternating load cycles of + and -47k, producing an alternating nominal stress of $\pm(47/50)(30.4 \pm 1.3)$ ksi, or $\pm$ 29.8 ksi, and $\pm$ 27.4 ksi, or an average stress of $\pm$ 28.6 ksi.

Following this test, two specimens of this original design were subjected to alternating loads until failure occurred.

The final study dealt with a specimen having a redesigned wing-plate arrangement. After a static loading sequence with maximum applied loads of + and -50k, the joint was subjected to alternating loads until failure occurred.

III-2. Static Load Results

III-2-1. Wing-Plate Joint (original design).—This joint was tested initially with increasing load steps of 5k, namely: P = 0k, -5k, 0k, +5k, 0k, -10k, 0k, +10k, 0k, -15k, 0k, +15k, 0k, and -20k, 0k, +20k and 0k. After this cycle, the load steps were increased with 10k values, and zero readings taken only after each complete cycle, namely:

-30k, +30k, 0k,
-40k, +40k, 0k, and finally
-50k, +50k, 0k.

During this last load cycle the wing-plates nearest to the horizontal member exhibited a distinct buckling deformation at P = -50k. Following the release of this load and the application of a load P = +50k, the buckle disappeared almost entirely after reducing the load again to 0k. The sequence of these observations is shown in Figure 6. It should be noted that this buckling was restricted to the wing-plates nearest to the horizontal member. This indicates a larger load in these wing-plates than in the two other plates.

In order to obtain data from which the elastic stress distribution could be determined accurately, a second series of step-wise increasing and decreasing loads in 10k intervals was applied and the data recorded. First, the load was increased step-wise up to -50k; after reducing this load in 10k steps to 0k, the same procedure was followed with a maximum load of +50k. The results of this phase of the study, as far as the elastic stresses are concerned, are shown in Figures 7 and 8 for maximum loads of P = -50k and +50k, respectively.

A general observation can be made after comparing the stresses on the diagonal tube wall near the column member under tension and compression. The results show very consistently that the stresses under a compressive diagonal force are higher in absolute values than those observed under a tensile force in the diagonal. This indicates that the load transferred directly from the diagonal member to the column seems to be higher under compression than under tension, or consequently, that the wing-plates transfer more load under tension than under compression. Hence, one can conclude that a certain non-linearity exists. This can be explained by recognizing the fact that under tension the cement grout fill near the center of the joint is not fully effective. Therefore, a transfer of loads towards the outside of the wing-plates will result. The stresses in the wing-plates, as shown in Figure 9, clearly show this same tendency with larger stress values under tension than under compression. The same is true for the stresses on the column wall along the welds between wing-plates and column wall. The general behavior is also clearly indicated in the actual load-strain plots shown in Figures 10 and 11.

The final load sequence on this first specimen was a continuation of step-wise increased load reversals; namely:

0. -50k, 0k, +50k, 0k
0. -60k, 0k, +60k, 0k, etc.

The earlier-observed buckling phenomenon was noticed at each step. At -70k all four wing-plates buckled for the first time. This led to a gradual deterioration of the joint. At a load of +90k, a small crack in the column wall near the toe of the diagonal member next to the horizontal was observed. At loads above -80k, a distinct crushing sound in the column section could be heard. After having been subjected to a load P of +100k, at which the earlier-noticed crack propagated over about 3 inches while opening up to about 1/8 inch, the specimen failed in compression at -110k. Reversing the load subsequently into tension resulted in a complete separation of diagonal and column wall at +80k.

After completion of the test, the interior of the column section in the vicinity of the joint was exposed. The grout immediately under the joint was crushed down to a depth of 6 inches. The interior $4\frac{1}{2}$-inch diameter pipes were flattened about 3/16 inch. The range of failure in the grout reached over the full extension of the wing-plates.

III-2-2. Non-Wing-Plate Joint.—The non-wing-plate connection was first subjected to a step-wise increased maximum negative load P of -40k. This load was subsequently reduced in 10k intervals until zero was reached. A similar upward and downward step-wise procedure was followed with a maximum positive load of +40k. The data recorded at each load step allowed an evaluation of the elastic stress distribution as shown in Figures 12 and 13. For comparative purposes, the stress values are presented for applied loads of - and +50k. The results clearly show that a substantial yielding occurs throughout the joint. Furthermore, there seems to be a tendency for the stresses in the diagonal tube wall farthest away from the plane of the truss to be in absolute values larger under tension than under compression. This phenomenon, as could be expected, seems to indicate a reduced efficiency of the grout-filled column section under tensile loads. This observation, which is similar in principle to that noted for the wing-plate joint, is further supported by the load-strain graphs presented in Figures 14 and 15.

An additional study carried out in this phase deals with the evaluation of the bending stresses in the column section due to the applied load. Therefore, 14 cross gages were placed along a normal section of the column member about 3 inches above the incoming horizontal branch member. These gages were predominantly positioned on one side of the truss plane. Two cross gages were placed on the opposite side for purposes of comparison. Figure 16 shows the experimental stress values for both positive and negative loads of 50k. The theoretical stress distribution in the same figure is based on a moment-carrying capacity of the steel section, neglecting the grout. However, these stresses will be reduced considerably if both the grout and the steel are assumed to resist the moment. The following analysis is hereby offered:

$$\text{Steel: } I_s = 1904 \text{ in}^4, \; E_s = 30 \times 10^3 \text{ ksi}$$

$$\text{Grout: } I_g = 11890 \text{ in}^4, E_g = 4 \times 10^3 \text{ ksi}$$

$$\text{Moment: } M = 35.75 \times P = 35.75 \times 50 = 1785 \text{ in.}$$

If both steel and grout resist the moment, then

$$M_s/E_sI_s = M_g/E_gI_g \text{ with } M_s + M_g = M.$$

Hence $M_s = 975\text{k in and } M_g = 810\text{k in.}$

Based on the above results, the maximum stress can be calculated for each case, namely:

a) neglecting grout participation: $f_s = (1785/1906)\ 12 = 11.2$ ksi,

and

b) including grout participation: $f_s = (975/1906)\ 12 = 6.1$ ksi.

Comparing these values with the experimental stresses near the branch connection, we can conclude that the wall in that vicinity behaves as if the grout is completely ineffective. However, on the far side of the section where the experimental stress values are 6.7 ksi and -6.3 ksi for P = -50k and +50k, respectively, the agreement between these values and the analytical stress value of 6.1 ksi seems to indicate that the stress value there can be calculated on the assumption of a complete moment resistant cross section. In general, it seems reasonable to state that the composite cross section can be assumed fully effective except in the immediate vicinity of joints.

The final phase of the static load program was carried out to establish the ultimate failure load. After applying successive loads of -50k and +50k, the applied load was brought to -60k and subsequently increased with 10k intervals to -80k. After reducing the load to zero, it was reversed and raised to +50k, +60k and +70k. Failure, due to a progressive separation of the diagonal from the column wall, was recorded at a load of +72k. Thus, as shown in Figure 17, failure developed first as a tearing of the column wall at the toe of the weld between the diagonal and the column next to the outer branch member. Due to this initial failure, the load in the diagonal had to be transferred almost exclusively through the welds on the outside of the tube. As a result, complete failure occurred by a successive tearing of the diagonal member wall all along the weld between this member and the column.

It should be noted that already under a compressive load P = -50k, an obvious crushing sound inside the column section had been observed. After cutting the column wall away, the grout area under the diagonal section was severely pulverized. The damaged area had locally the same depth, but was rather small compared with that observed after failure of the first specimen tested. Figure 18 shows the damaged grout after removal of the crushed and broken pieces. The inner pipe sections were undeformed in this case.

III-2-3. Wing-Plate Joint (modified design - Figure 3).—This specimen was tested under static loads in order to evaluate the distribution of the diagonal member force in the transfer to the wall of the column member. Therefore, the instrumentation was concentrated in the throat section of the wing-plates and on both sides of the eccentric wing-plate stiffener. The applied load P was increased and subsequently decreased in 10k intervals for both positive and negative values of P, causing respectively tension and compression in the diagonal member. The maximum applied loads were P = -60k and +60k. The strain data over these load ranges showed a linear response in each instance.

The results, which substantiated the earlier findings, indicated that in case of a compressive force in the diagonal, 45% of the load is tranferred through the wing-plates. However, for a tensile force in the diagonal, the transferred load percentage is 65%.

Under the compressive load transfer, 30% is carried by the two wing-plates adjacent to the horizontal branch member, while the remaining 15% is carried by the two other wing-plates. In the case of a tensile load transfer, these percentages are 40% and 25%, respectively.

It is of interest to consider in detail some of the results obtained for loads of P = -40k and +40k. The corresponding diagonal force due to those loads is - and +90.4k, respectively. Table I presents the experimental values for the normal loads in the throat sections of the two wing-plates and in the associated stiffeners. Because of the joint symmetry, the total normal load in all four wing-plates under compression is -(2 x 22.6k) = -45.2k. This represents, resolved, an axial diagonal member force of 0.9 x (-45.2k) = -40.7k or 45% of -90.4k. Similarly, the total percentage under tension can be evaluated as 65%. Hence, the percentage of the diagonal load transferred directly to the column member wall is 55% in compression and 35% in tension.

TABLE I

LOAD DISTRIBUTION FOR P = ± 40k

Load P	Wing-Plate 1*		Wing-Plate 2**		Σ load
	Wing-Plate	Stiffener	Wing-Plate	Stiffener	
-40k	-13.6k	-1.5k	-6.6k	-0.9k	-22.6k
+40k	+18.3k	+2.1k	+10.8k	+1.8k	+33.0k

*wing-plate next to horizontal
**wing-plate away from horizontal

For design purposes it is useful to express the normal wing-plate forces and stiffener forces directly in a percentage of the diagonal member force. This evaluation, based on the load values shown in Table I, is presented in Table II.

TABLE II
NORMAL FORCES IN PERCENT OF DIAGONAL MEMBER FORCE

Diagonal Load	Wing-Plate 1		Wing-Plate 2	
	Wing-Plate	Stiffener	Wing-Plate	Stiffener
-100	-15.0	-1.5	-7.5	-1.0
+100	+20.0	+2.5	+12.0	+2.0

The normal, practically linear stress distribution in the wing-plates across the throat section shows invariably high stresses near the free edge of the wing-plates. The following in-plane stress distribution was observed:

for wing-plate 1: $\sigma_{max} = \sigma_{av} \pm 0.2\, \sigma_{av}$, and

for wing-plate 2: $\sigma_{max} = \sigma_{av} \pm \sigma_{av}$, where

σ_{av} = Force /(throat cross section of plate).

Hence, the normal stresses across the throat section of wing-plate 1 vary between 0.8 σ_{av} and 1.2 σ_{av}, with the maximum value occurring near the free edge and the low value in the corner of the wing-plate near the column wall and diagonal tube. For wing-plate 2, the extreme values vary between a maximum of 2 σ_{av} near the edge and zero near the corner. The average axial stresses for the eccentric stiffeners on wing-plates 1 and 2 are 0.5 σ_{av} and 0.8 σ_{av}, respectively.

In addition to the above "longitudinal" in-plane stresses, the throat section is also subjected to "longitudinal" and "transverse" (parallel to the section) bending stresses. These stresses are quite uniform across the section and are, for wing-plate 1, respectively, ± 1/8 σ_{av} and ± 1/4 σ_{av}. For wing-plate 2, these stress values are, respectively, ± 1/5 σ_{av} and ± 1/3 σ_{av}. The transverse in-plane stress is negligibly small.

The static load tests on this specimen were completed after a study of the load symmetry indicated an excellent agreement between comparative strains at selected points in all four wing-plates.

<u>III-2-4. Wing-Plate Joint (revised design - Figure 4)</u>.—Because the stresses in wing-plate 1 or the modified joint were about twice as large as those recorded in wing-plate 2, it was decided to increase the plate thickness of plate 1 from 1/8 inch to 3/16 inch. Although it was realized that, due to the larger stiffness, the increased thickness would tend to draw more load to this plate, it was hoped that the final result would show a reduction in stress. Based on the above considerations, a revised design of the wing-plate connection—as shown in Figure 4—was developed and tested.

In order to evaluate the load transfer and stress distribution in this joint, a total of 140 gage circuits, grouped in 12 rosettes and 52 cross gages, was placed on this specimen. These gages were concentrated on one side of the joint only. Gages on the two wing-plates were located on both sides of each plate along the throat cross section and along the weld between plate and column member. The gages on the outside of the diagonal tube wall were all cross gages and were located in 180° arc sections along 7 cross sections. Figure 19 shows schematically the locations of the several instrumented sections.

The applied load P was again step-wise increased and decreased to maximum values of +50k and -50k, respectively. The load intervals were invariably 10k. Three load cycles were carried out. After a relatively small initial non-linearity had been observed in the first cycle, the subsequent load-strain data showed an excellent linearity for both the tensile and compressive portion of the loading cycle.

A study of the stress values on both sides of each of the wing-plates reveals that for a tensile force in the diagonal, 64% of that force is transferred to the column by means of the wing-plates. In the case of a compressive force in the diagonal, this percentage is 57%. The specific normal stress values as computed from the strain data and the suggested in-plane stress distribution for P = ± 50k are presented in Figure 20. According to the assumed stress distribution, the loads carried by plate 1 under tension and compression are +31.3k and -27.6k, respectively. These values include +4.3k and -4.2k, respectively, for the load transferred through the edges stiffener. For plate 2, the total loads transferred under tension and compression are only +8.7k and -7.9k, respectively. These values include +2.4k and -2.3k for the stiffener loads.

Table III presents the experimental values for the normal loads, in the two wing-plates and the associated stiffeners.

TABLE III
LOAD DISTRIBUTION FOR
P = ± 50k

Load P	Wing-Plate 1		Wing-Plate 2		Σ load
	Wing-Plate	Stiffener	Wing-Plate	Stiffener	
-50k	-23.4k	-4.2k	-5.6k	-2.3k	-35.5k
+50k	+27.0k	+4.3k	+6.3k	+2.4k	+40.0k

Resolving the above loads into a resulting force parallel to the diagonal axis, the following percentage values of load-transfer with respect to a diagonal force of 113k result:

Compression:	Total:	2 [27.6 + 7.9] x 0.9 = 63.9k or	57% of 113k
	Plate 1:	(one only)	22½%
	Plate 2:	(one only)	6%
Tension:	Total:	2 [31.3 + 8.7] x 0.9 = 72k or	64% of 113k
	Plate 1:	(one only)	25%
	Plate 2:	(one only)	7%

These percentage values indicate that under compression and tension, respectively, 43% and 36% of the diagonal force is transferred directly to the column member.

For purposes of design, the loads indicated in Table III can be expressed in percentages of the diagonal member force. Table IV presents the computed percentage values for both compression and tension loading.

TABLE IV
NORMAL FORCES IN PERCENT OF
DIAGONAL MEMBER FORCE

Diagonal Load	Wing-Plate 1		Wing-Plate 2	
	Wing-Plate	Stiffener	Wing-Plate	Stiffener
-100	-21.0	-4.0	-5.0	-2.0
+100	+24.0	+4.0	+5.5	+2.0

The above results indicate that increasing the plate thickness of wing-plate 1 indeed draws more load to this plate than before, namely 22.5% versus 15% under compression and 25% versus 20% under tension. Nevertheless, the maximum stresses were reduced, as intended, by approximately 15 to 20%. Significant in this study also is the fact that the earlier difference of 20% between the total transfer percentages under tension and compression (+65% and -45%) has been reduced to only 7% (+64% and -57%). This indicates a more uniform behavior of the joint under alternating loads. The reason for this phenomenon seems to be the increased stiffness of wing-plate 1, which attracts a predominant portion of the total load (+50% and -45% for plates 1 versus +14% and -12% for plates 2). Furthermore, the effect of this wing-plate in stiffening the column wall must have contributed to the observed force concentration.

In regard to the stress distribution along the welds between wing-plates and column member, it is interesting to note that the calculated stress—as shown in Figures 21 and 22— is very consistent with the earlier evaluated load-transfer distribution through the wing-plates.

Finally, it is of interest to observe the stresses calculated for the gages located on the diagonal tube wall along sections 1 through 7, as shown in Figure 19. The stress values are presented in Figures 23 and 24. These stress values are not necessarily representative for the membrane stresses, although beyond the immediate stress concentration areas (as near the wing-plate tips) one can assume that local bending will not be very significant. On the basis of this hypothesis, it is of interest to evaluate the total force in section 6 for both compression and tension. While assuming a linear stress variation between the points with calculated stress values, the total compressive and tensile forces in that section are, respectively, -42% and +35% of the basic diagonal member force of 113k. In comparing these percentages with the corresponding values of -43% and +36%, as previously evaluated from the wing-plate studies, we note an extremely close agreement. Percentage values for other sections are presented in the same figures.

III-3. Alternating Load Results

III-3-1. Wing-Plate Joint (original design).—Although this joint was tested after the joint with the modified wing-plate design had been studied, the response of the original joint under alternating loads is presented first. The applied load P was erroneously increased to + and -60k rather than + and -47k, which would have corresponded with an average nominal stress in the diagonal of ± 28.5 ksi. Although this higher load has undoubtedly caused an earlier failure than could have been expected under the intended load of ± 47k, the overall response would probably not have been significantly different.

The following failure phenomena were observed and are presented in Figure 25:

@ 200 cycles:	buckling of all wing-plates under compression, with wing-plates 1 showing a 1/4-in. out-of-plane buckle, and wing-plates 2 a 1/8-in. buckle.
@ 210 cycles:	crack in plate 1-a starting at A and extending over a length of 1/4 in. along the weld towards B.
@ 220 cycles:	crack in plate 1-b starting at E and extending over a length of 1 in. towards F.
@ 580 cycles:	abrupt failure in plate 1-b along GH, followed by a propagation of the crack along the weld HF.
@ 620 cycles:	sudden crack in wall of diagonal over a 1.5-in. distance between C and D. After 635 cycles this crack length was 5 in. After 645 and 663 cycles the crack had propagated to a total length of 8 and 9.5 in., respectively.

The test was stopped after 663 cycles. It can be expected that under a load of ± 47k, failure would have occurred in the tube wall near point A. Under subsequent loading rapid crack propagation towards C and D can be expected. Based on recent fatigue studies [3], first crack failure under a load of ± 47k could probably have been expected after approximately 500 cycles.

[3] Bouwkamp, J. G., Stephen, R. M., Tubular Joints Under Alternating Loads, Report No. 67-29, November 1967, Structures and Materials Research, Department of Civil Engineering, University of California, Berkeley.

III-3-2. Non-Wing-Plate Joint.—This joint was correctly subjected to an alternating load of + and -47k. Failure occurred abruptly in the wall of the diagonal tube immediately above the toe of the weld near the horizontal web member. This crack started almost immediately, and had, after 19 cycles, propagated 5 inches to either side of the diagonal along the weld between diagonal and column. Such a failure is entirely in line with the severe stress distribution noted before in section III-2-2 for an identical specimen.

III-3-3. Modified Wing-Plate Joint.—An original wing-plate specimen was modified by the addition of little triangular plates near the wing-plate tips and by stiffeners placed eccentrically on the outside of each wing-plate (see Figure 26).

The joint was subjected to an alternating load of + and -47k, with a typical speed of 14 cpm. The following failure phenomena were observed and are illustrated in Figure 26:

@ 1750 cycles: A crack developed in plate 1-b along the weld at point D. After 1850 cycles this crack had propagated 0.5 in. towards E. After 2880 cycles the crack had reached the weld between diagonal and wing-plate.

@ 1800 cycles: A crack similar to that noted above developed in plate 1-a at point A. This crack had propagated after 2900 cycles entirely along the weld AB.

@ 2900 cycles: A 0.5-in. crack along the weld between diagonal and wing-plate was noted in plate 1-b.

@ 2900 cycles: (cont'd.) The following crack propagation from E to F was observed:

@ 8700 cycles, 1.5 in.
@ 9000 cycles, 2.0 in.
@ 9550 cycles, 2.5 in.
@ 11950 cycles, 3.0 in.

@ 5000 cycles: A crack in wing-plate 1-a was observed and propagated from B to C. The following crack propagation was noted:

@ 6400 cycles, 0.5 in.
@ 8450 cycles, 1.0 in.
@ 9340 cycles, 2.0 in.
@ 9850 cycles, 2.5 in.
@ 10950 cycles, 3.0 in.

@ 5270 cycles: A crack developed in the wall of the diagonal at point G and propagated towards point H as follows:

@ 6700 cycles, 0.75 in.
@ 8700 cycles, 1.25 in.
@ 10950 cycles, 1.50 in.

In addition to the above cracks, failure also occurred in the diagonal tube wall above the weld between the diagonal and column member at a point nearest to the horizontal branch member. This crack was first observed after 4100 cycles. After 6800, 8700, 8800 and 10,950 cycles, the crack had propagated symmetrically to two sides and had reached a total length of 1, 1.25, 1.50, and 2 inches, respectively.

The test was terminated after 11,400 cycles of alternating load had been applied.

III-3-4. Revised Wing-Plate Joint.—This joint was subjected to an alternating load of + and -47k. Failure came suddenly after 800 cycles and progressed rapidly during the next 1000 cycles. The failure occurred simultaneously in the diagonal tube wall at points A and B above the tip of the wing-plates 1-a and 1-b (see Figure 27). The wall near point B was probably more critically stressed than point A, and thus exhibited a rapid crack propagation. After 1500 cycles the entire crack length CD was 2 inches. The subsequent crack propagation, which was very symmetrical, occurred as follows:

@ 1631 cycles, 2.5 in.
@ 1678 cycles, 3.0 in.
@ 1765 cycles, 4.0 in.
@ 1835 cycles, 6.0 in.

The results clearly indicate that the increased stiffness of wing-plates 1-a and 1-b caused an early failure due to increased stress and strain concentrations. It seems that the original wing-plate thicknesses are far more appropriate despite the high stresses occurring in these plates. These test results once more emphasize the significance of proper stiffness distribution in tubular joints.

IV. CONCLUSIONS

The wing-plate type of joint proved to be very effective in transferring loads to a thin-walled column section filled with a cement grout to increase the radial stiffness of that member. Static tests indicated that as much as 25% of the diagonal member load can be transferred through a single wing-plate. It can safely be assumed that a joint of the type tested with wing-plates of 1/8-inch thickness and stiffeners as shown in Figure 4 will resist at least as many load cycles at a nominal design stress level in the diagonal as any conventional in-plate gusset plate joint. A proper taper towards the diagonal of the plates with a length-to-width ratio of 2 will undoubtedly increase the fatigue life of such a joint. That the thin (t = 0.01 O. D.) column wall with cement grout fill backing can resist the high load transfer from the wing-plates to the column wall is found to be most satisfactory. This fact, as in so many other cases, has moved the critical design area towards the junction between wing-plates and web members.

In order to obtain in a wing-plate joint an identical load transfer between the member forces under both tension and compression, it is advisable to use a self-expanding cement grout which creates a pretensile hoop stress in the column member. This will probably assure complete contact between steel wall and core in order to obtain a truly effective supporting action through the entire load range.

As far as the bending stiffness of the entire column is concerned, tests indicated that one can assume a fully effective composite section, except in the immediate vicinity of a branch member connection.

Joints with a grout-filled column member and a wall thickness of 0.01 O. D., but without wing-plates, should never be used in the design of joints to be subjected to cyclic loads.

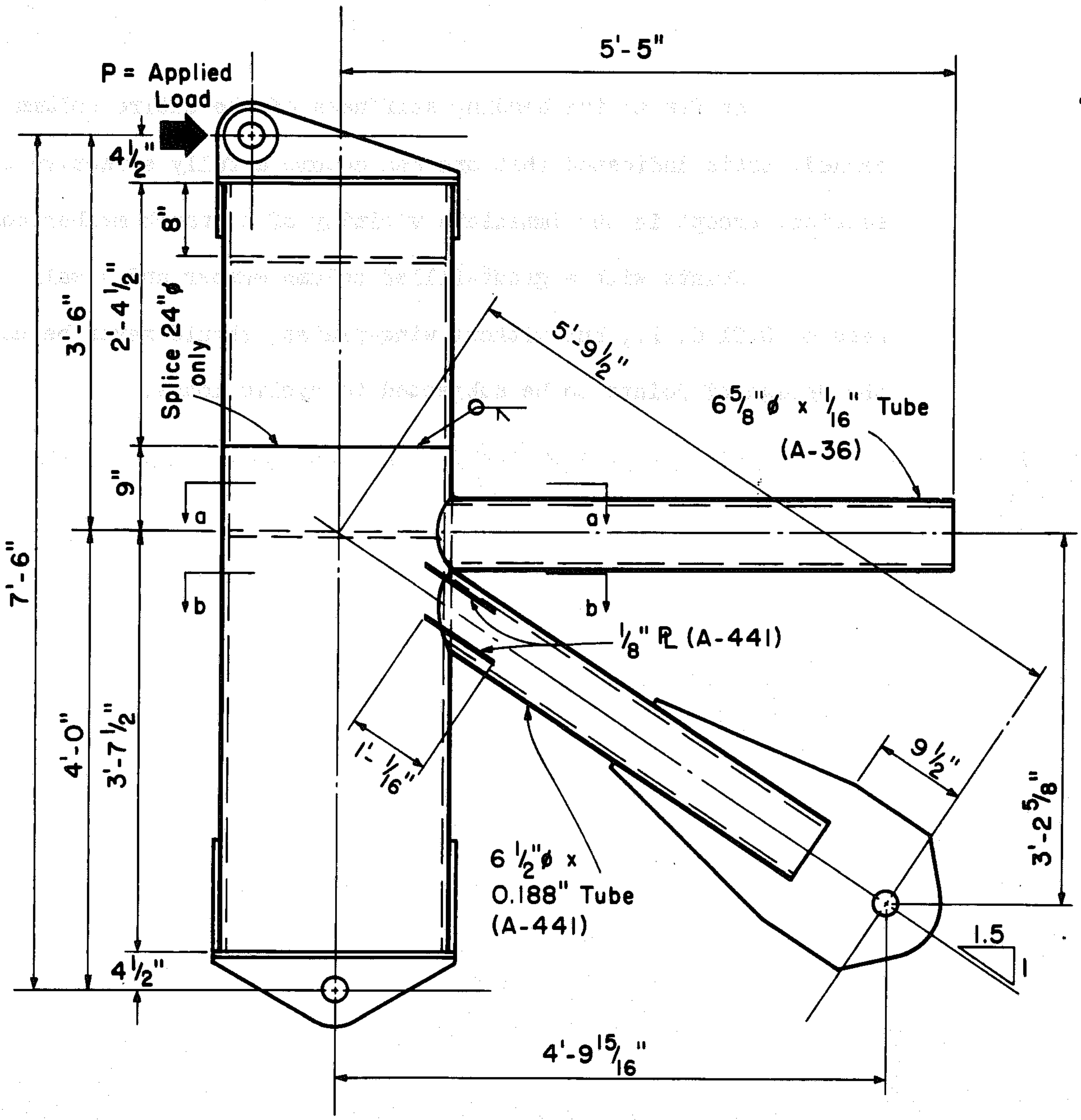

FIG. 1. MODEL JOINT ELEVATION.

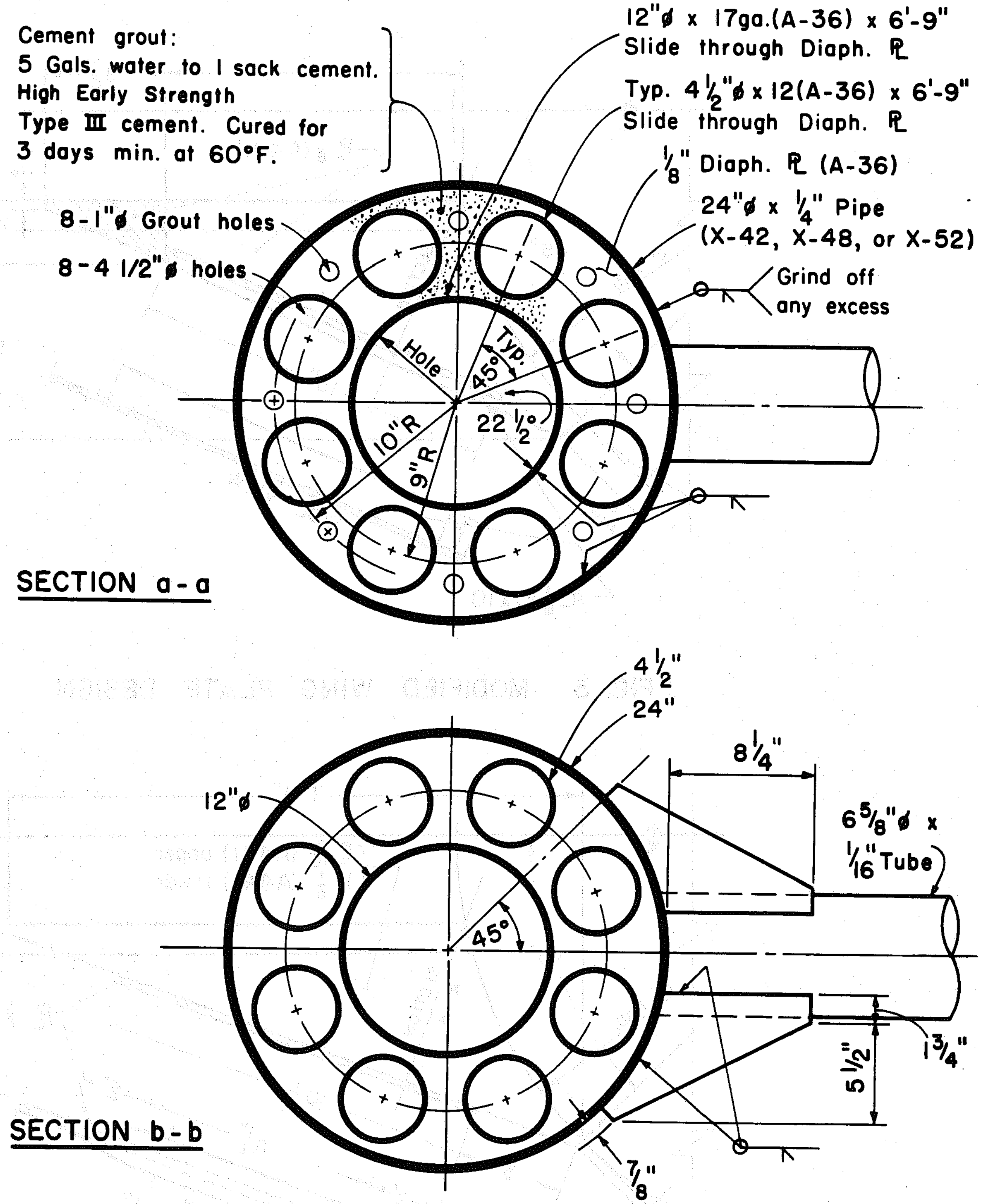

FIG. 2. MODEL JOINT.

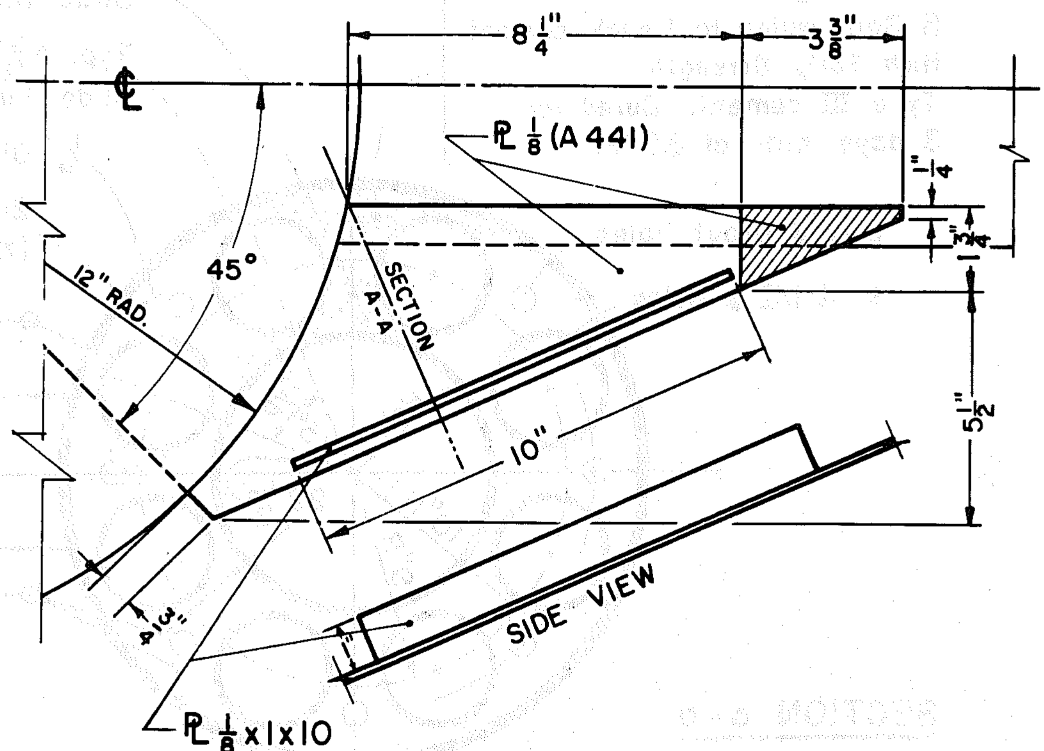

FIG. 3 MODIFIED WING PLATE DESIGN

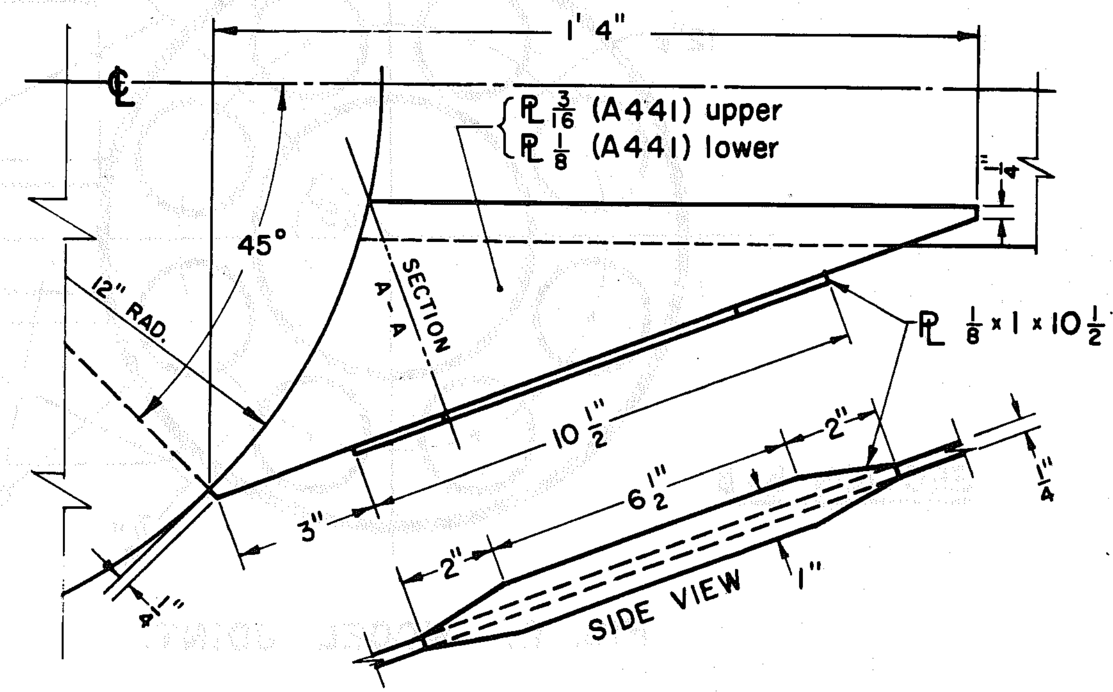

FIG. 4 REVISED WING PLATE DESIGN

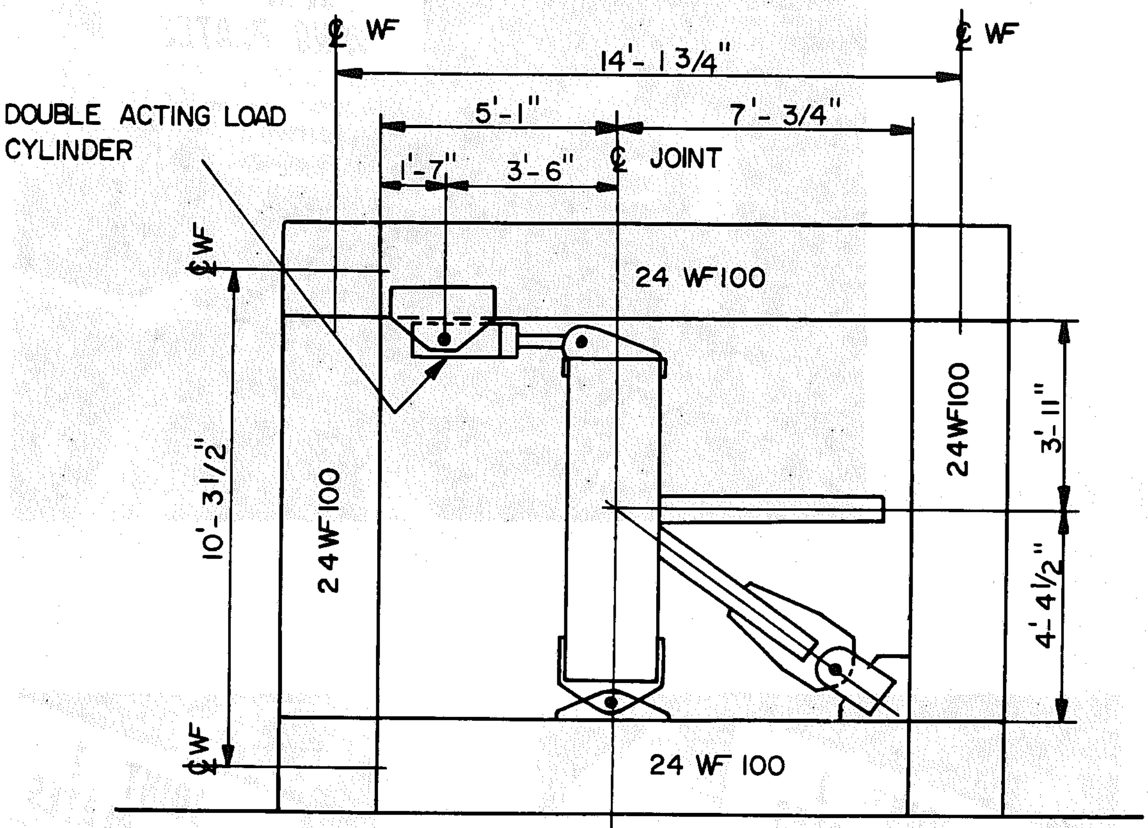

LOADING FRAME

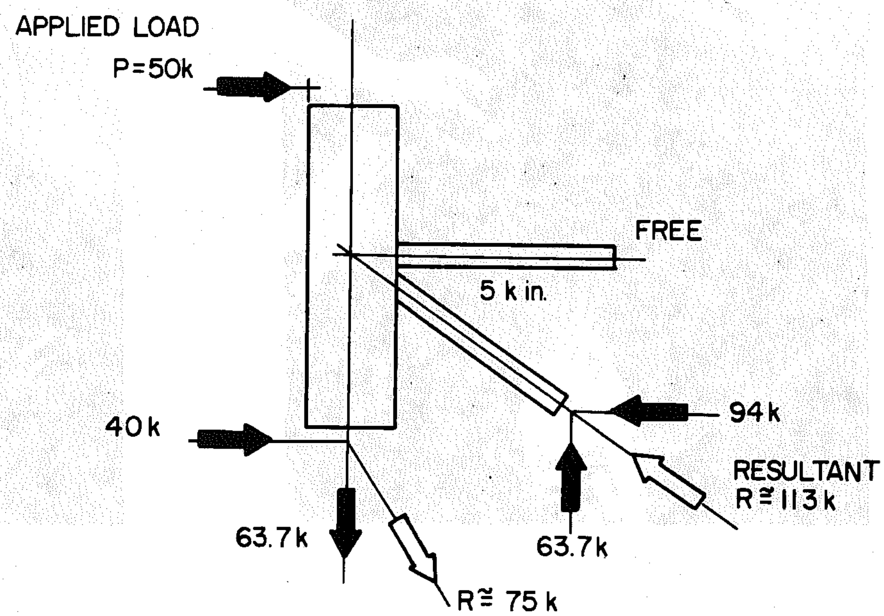

FORCE DIAGRAM

FIG.5 LOADING FRAME AND FORCE DIAGRAM

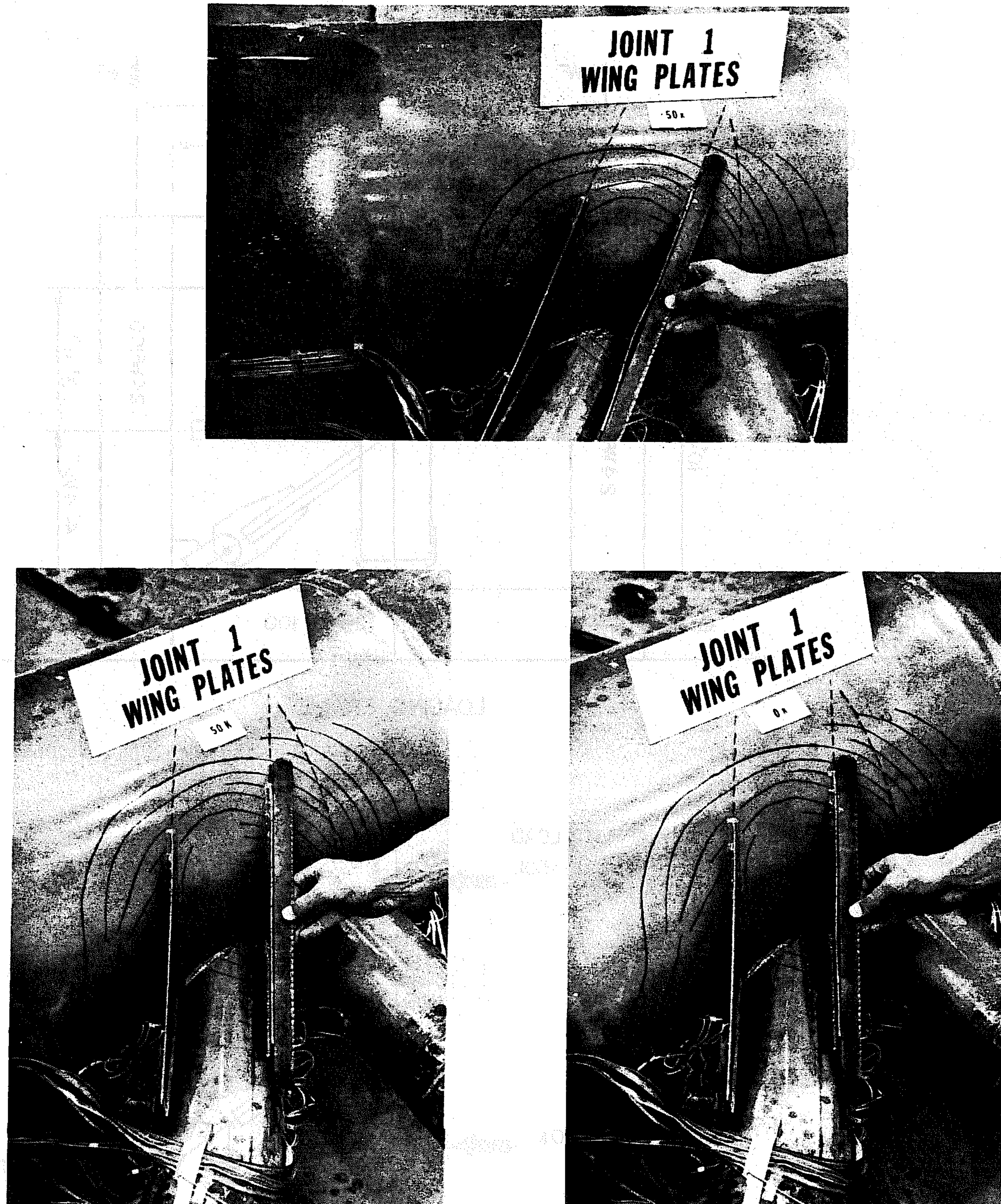

FIG. 6 DEFORMATION SEQUENCE AT P=-50k,+50k AND 0k

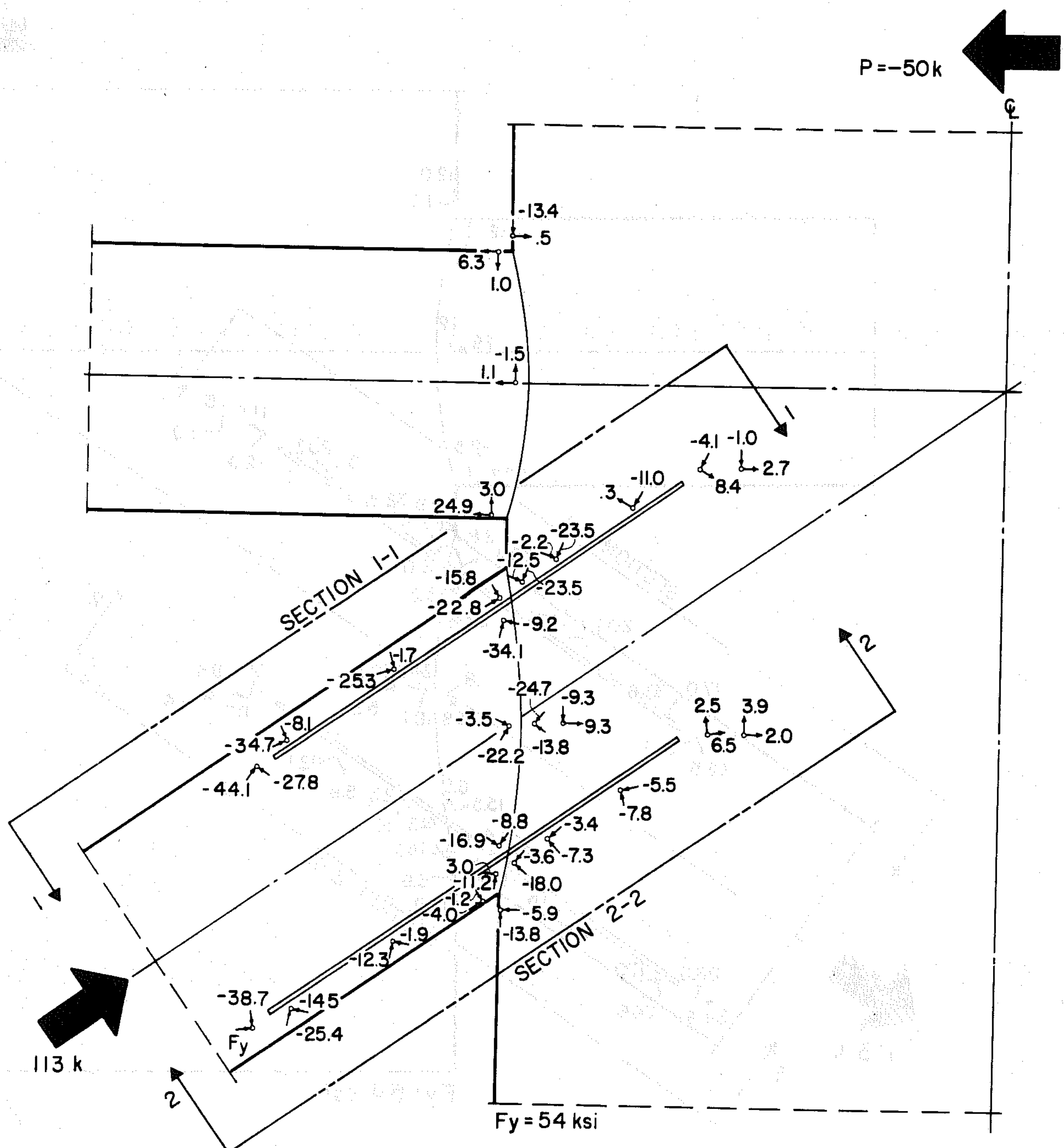

FIG. 7 SPECIMEN No. 1
STRESSES IN KSI AT P = -50 k

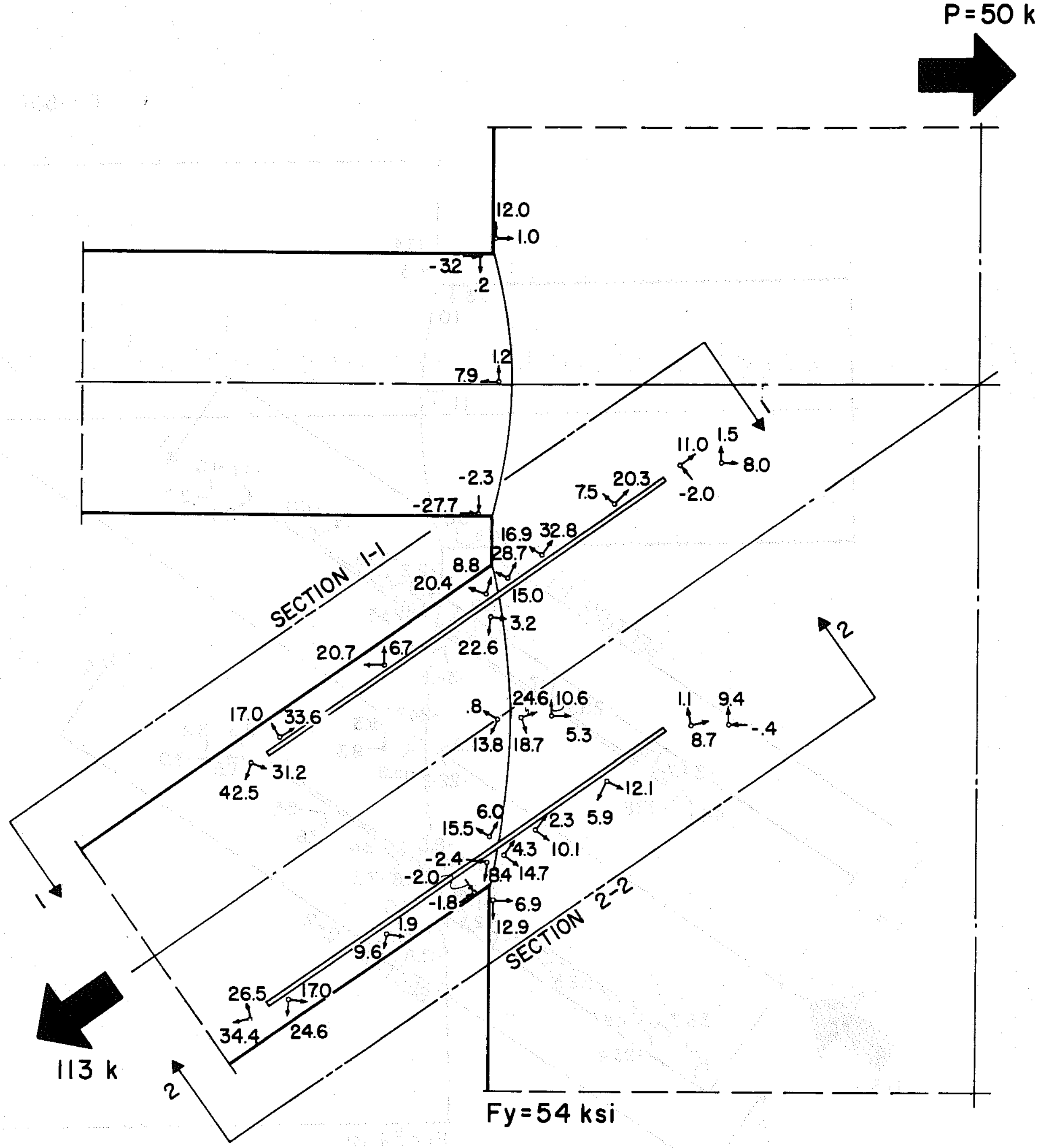

FIG. 8 SPECIMEN Nº 1

STRESSES IN KSI AT P = +50 k

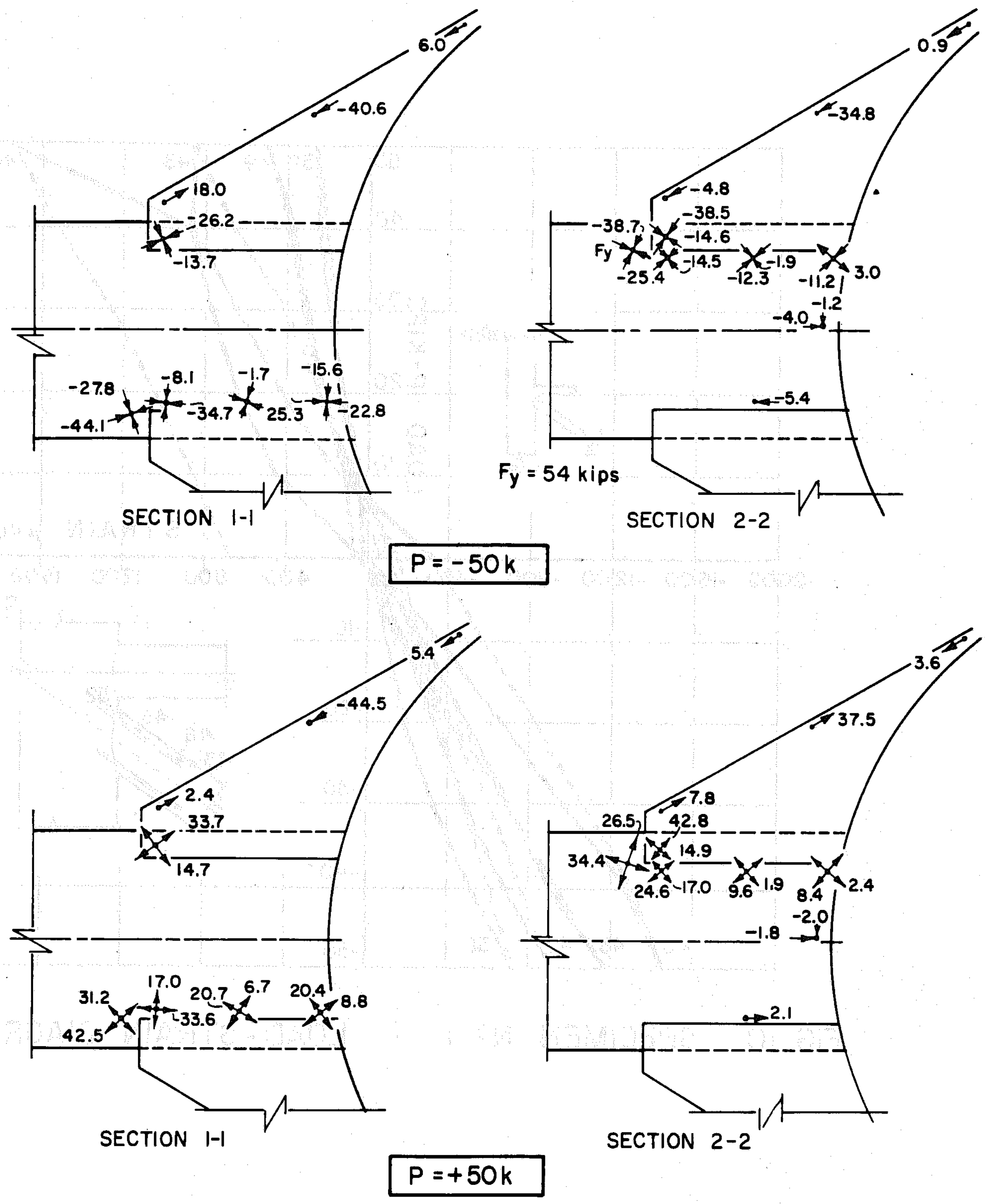

FIG. 9 SPECIMEN No. 1, STRESSES IN KSI

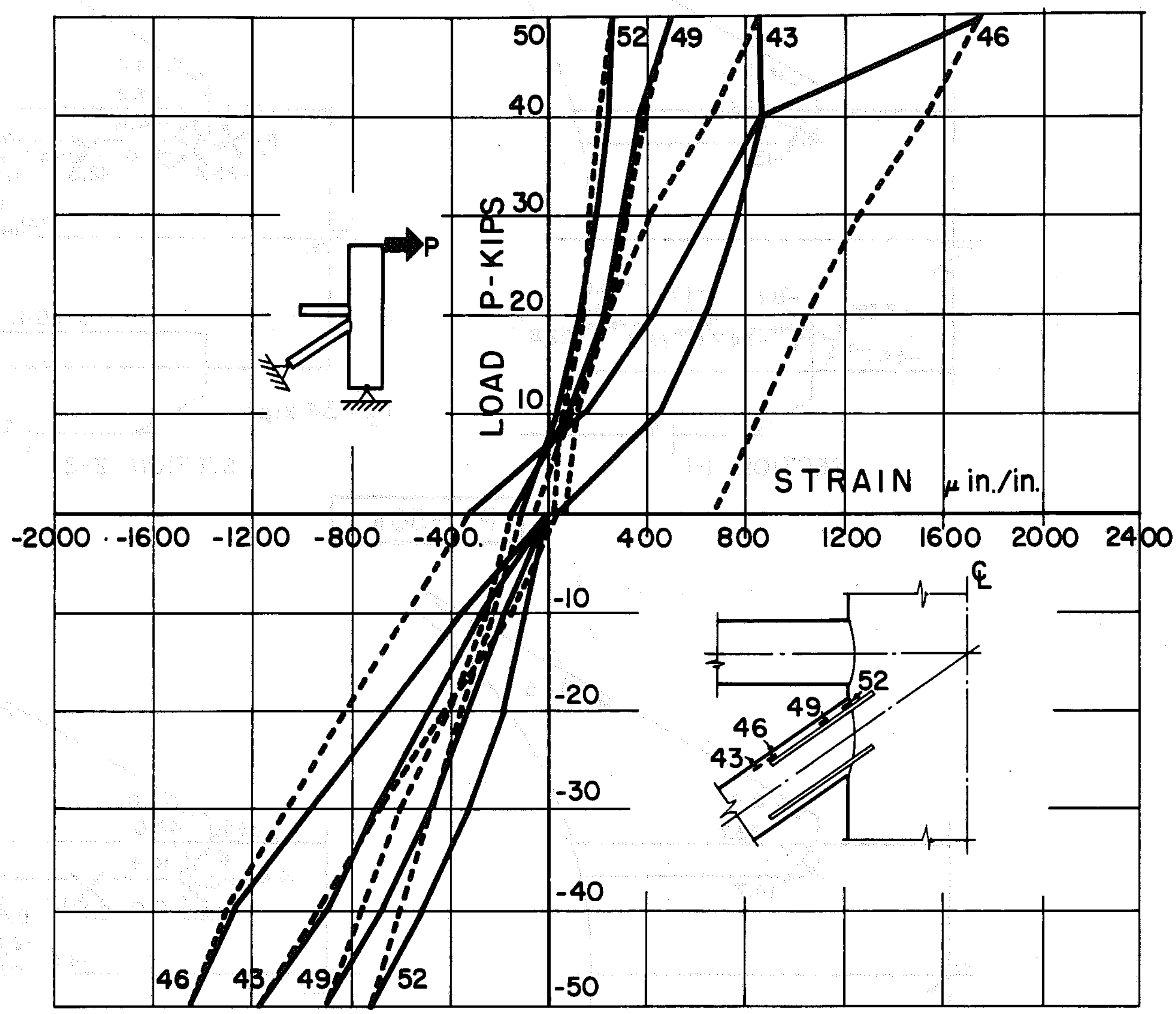

FIG. 10 SPECIMEN Nº 1 · LOAD-STRAIN DIAGRAM

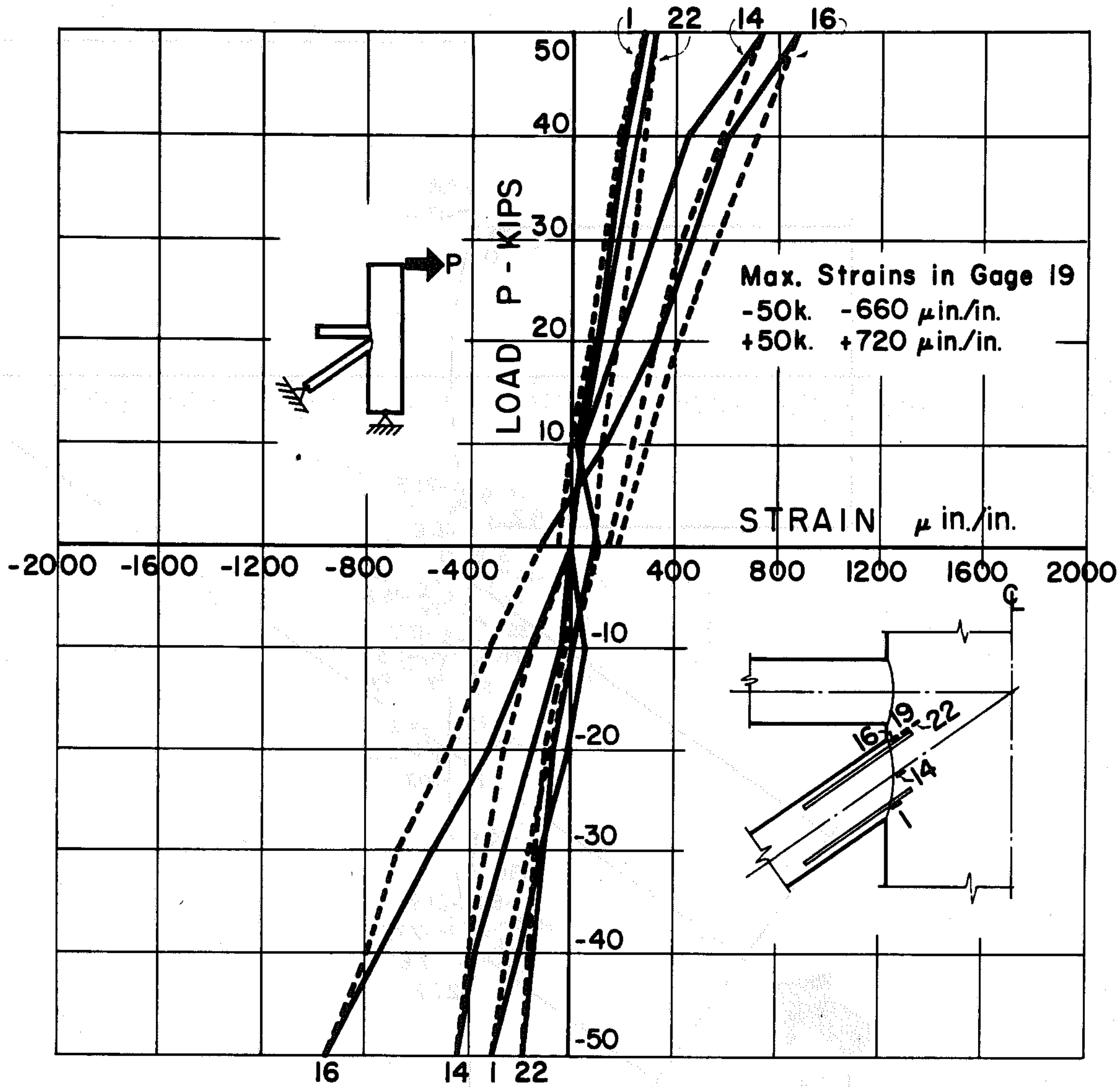

FIG. 11 SPECIMEN Nº 1 · LOAD-STRAIN DIAGRAM

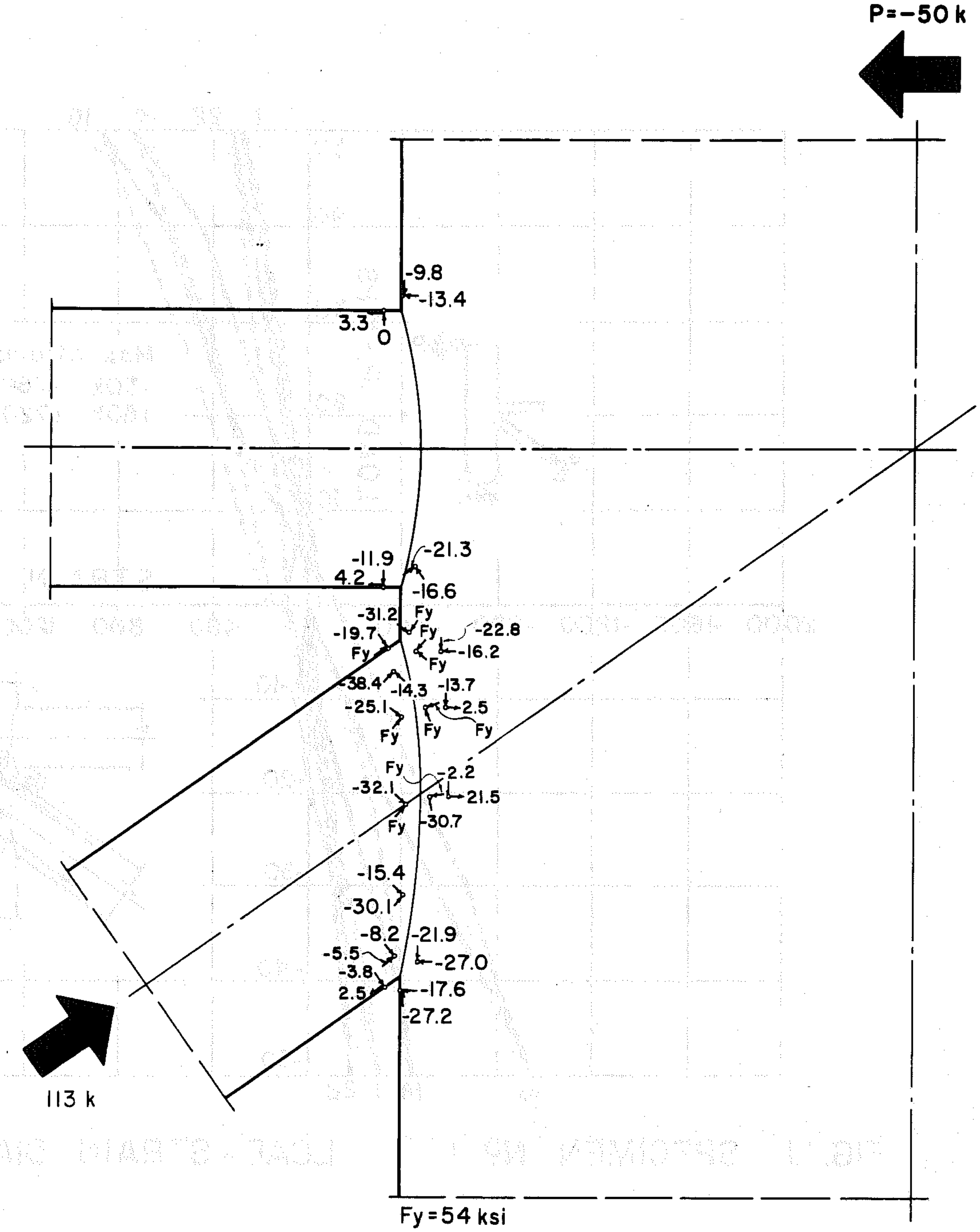

FIG. 12 SPECIMEN No 2

STRESSES IN KSI AT P= -50 k

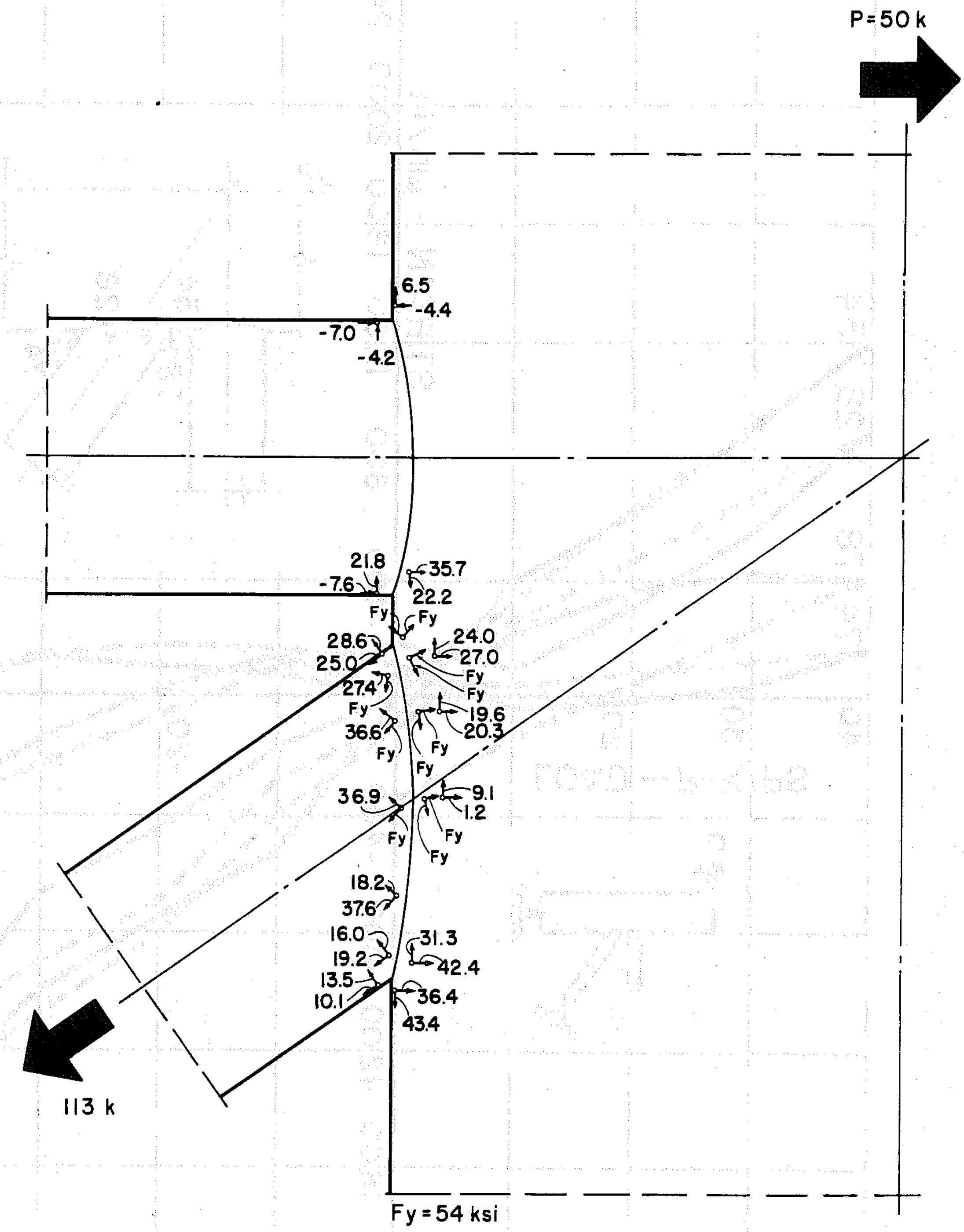

FIG. 13 SPECIMEN Nº 2

STRESSES IN KSI AT P=+50k

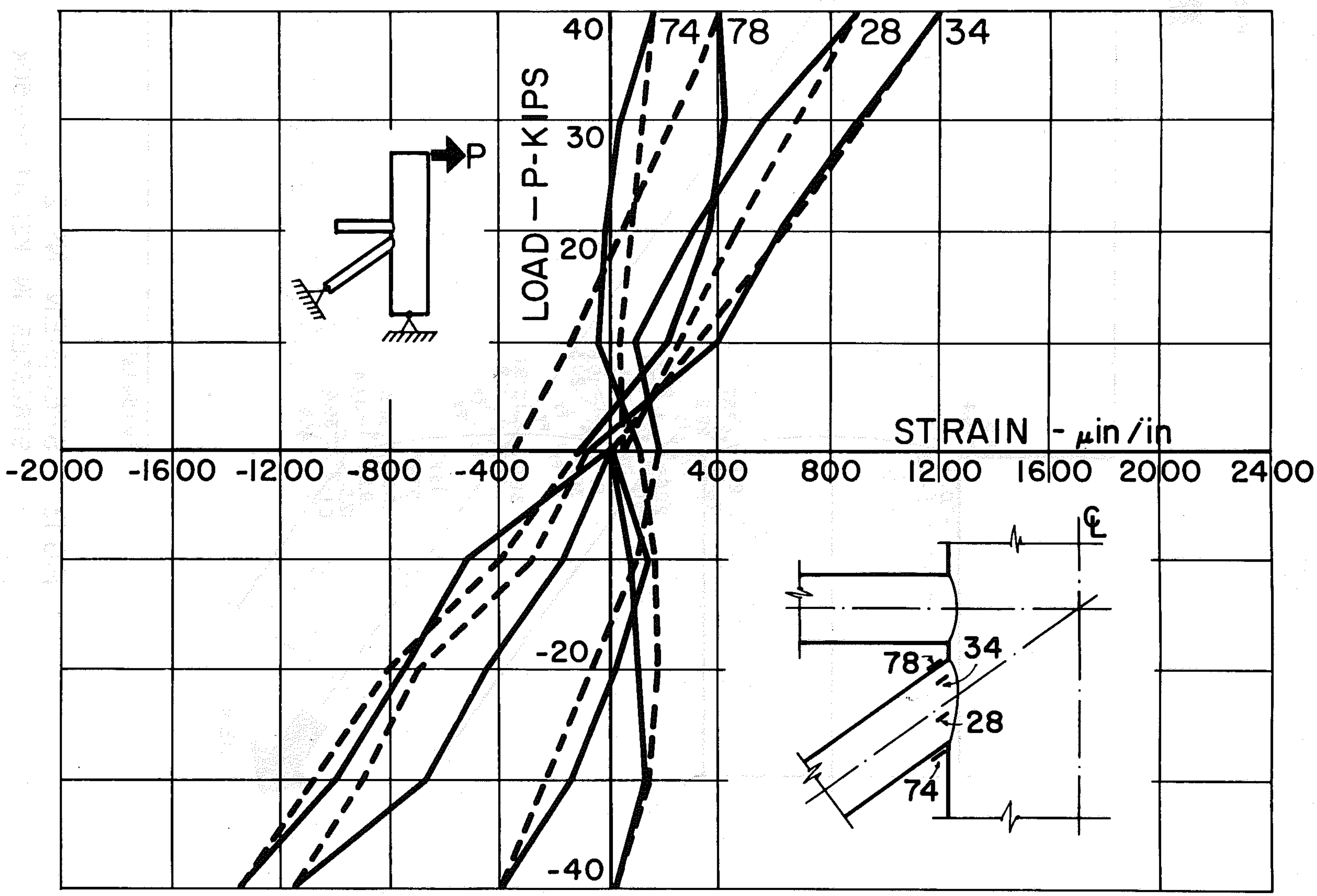

FIG. 14 SPECIMEN № 2 · LOAD-STRAIN DIAGRAM

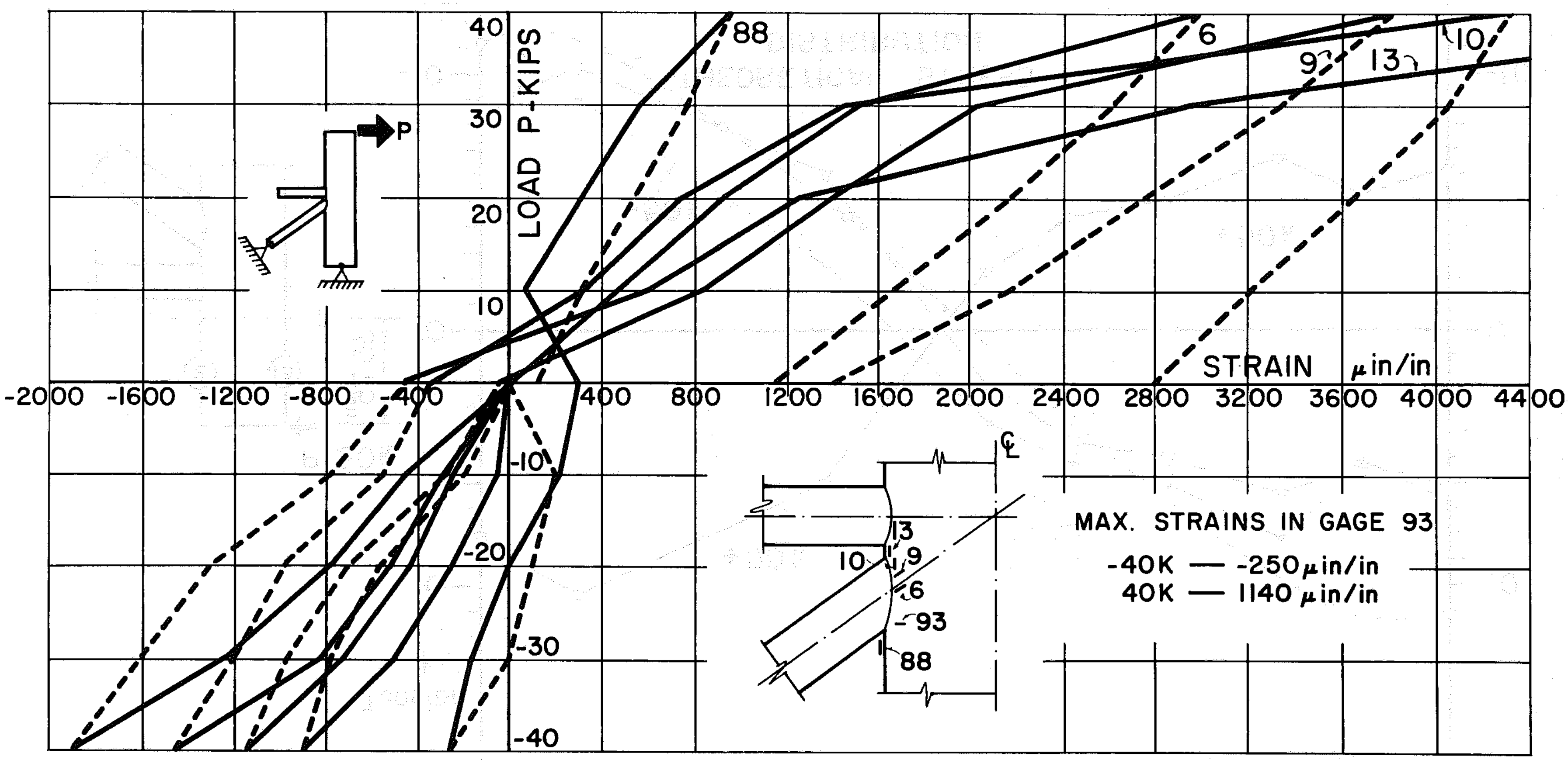

FIG. 15 SPECIMEN Nº 2 · LOAD-STRAIN DIAGRAM

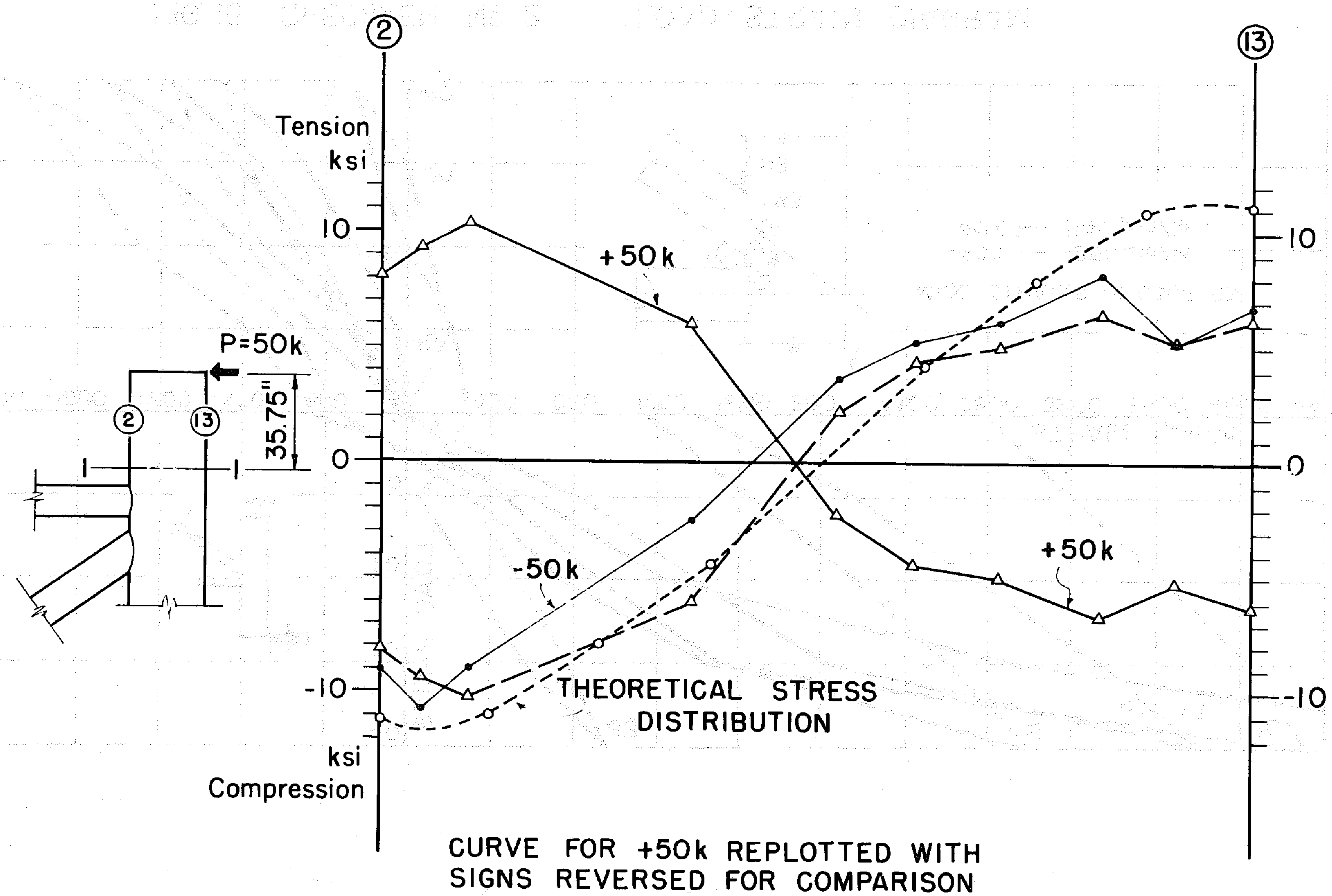

FIG.16 SPECIMEN Nº 2 · BENDING STRESSES IN SECTION I-I

FIG. 17 STATIC LOAD FAILURE (P=+72 k)

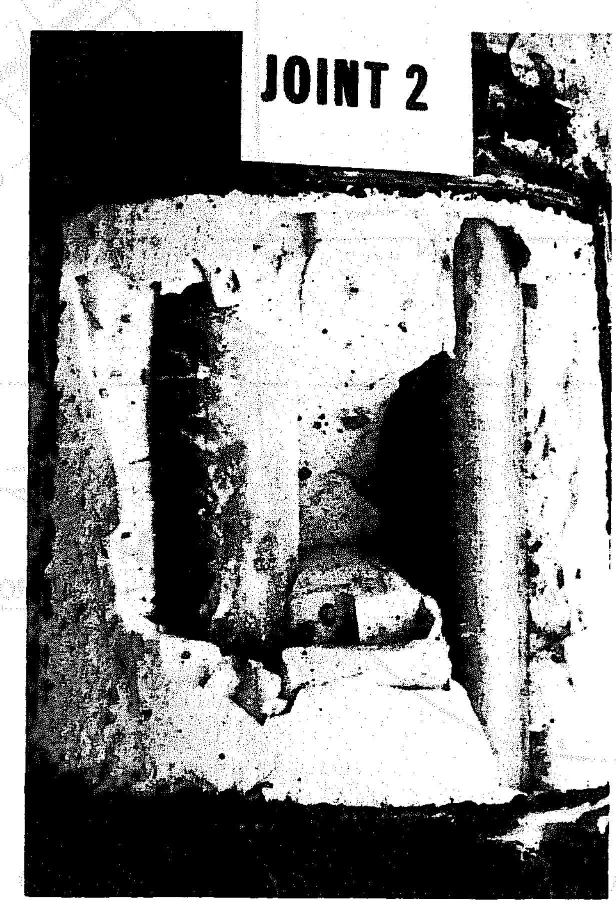

FIG. 18 INTERIOR GROUT DAMAGE

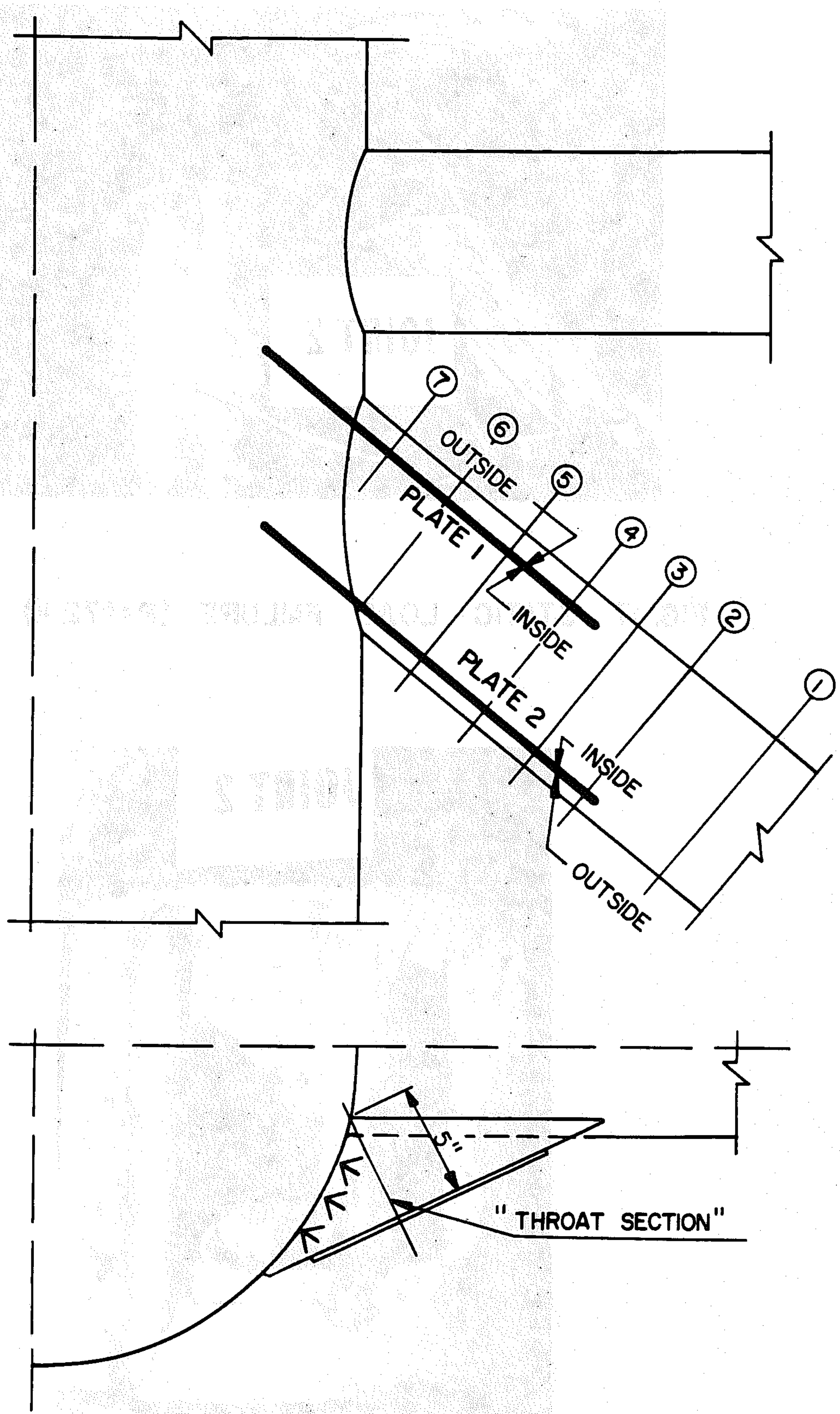

FIG. 19 INSTRUMENTED SECTIONS-REVISED WING PLATE DESIGN

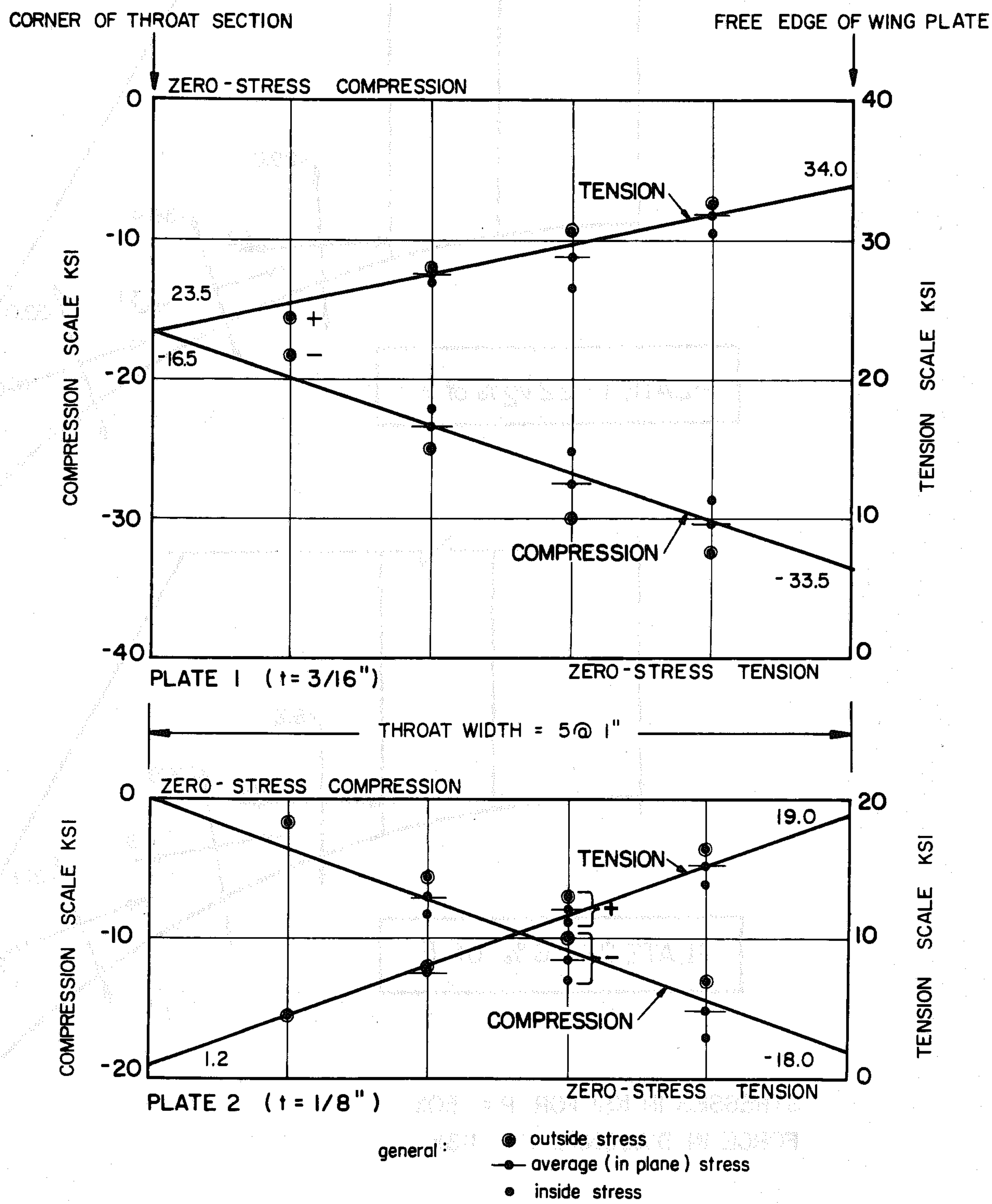

FIG. 20 STRESS DISTRIBUTION IN THROAT SECTION OF WING PLATES DUE TO P= ± 50k

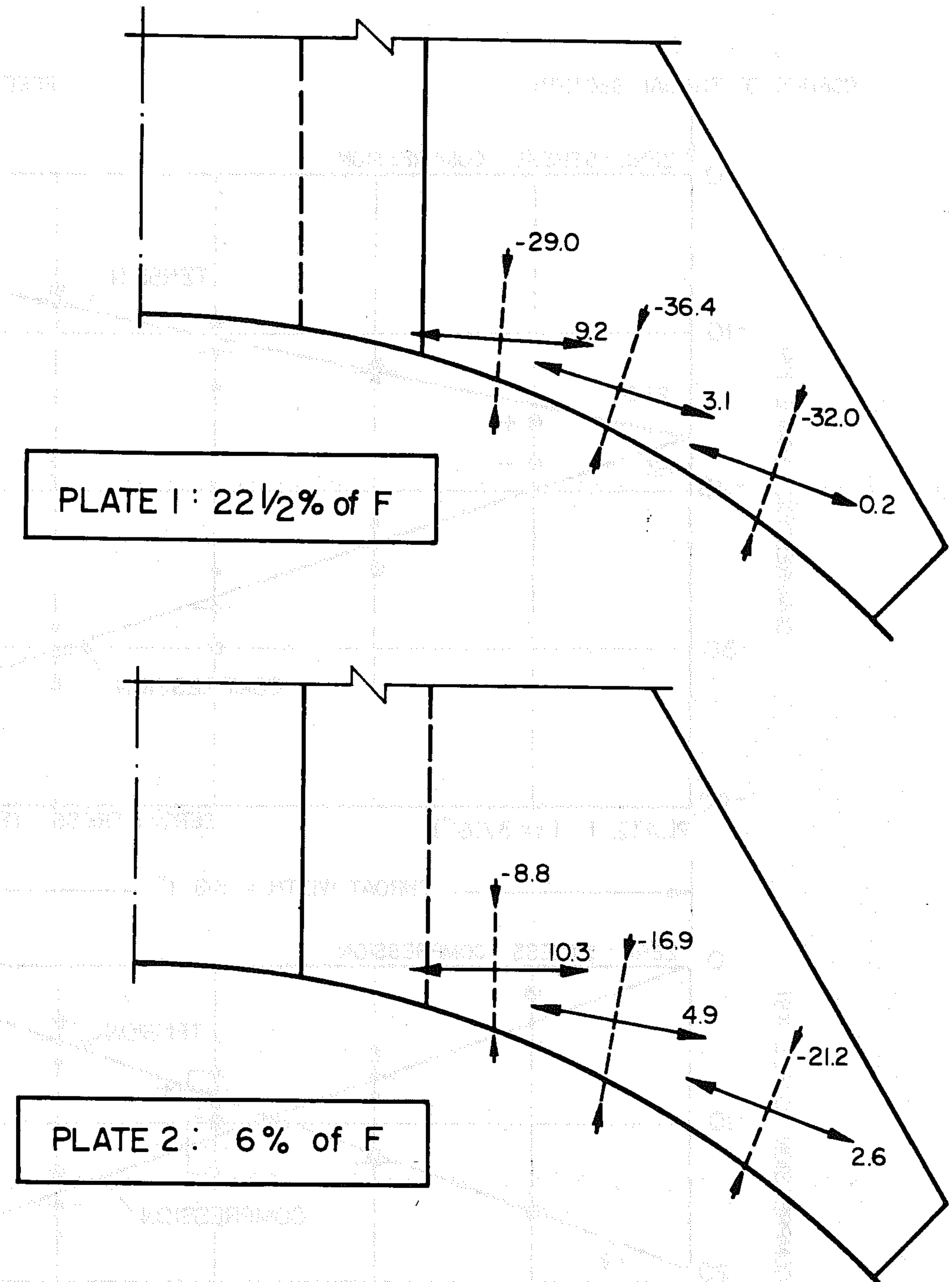

STRESSES IN KSI FOR P = -50k
FORCE IN DIAGONAL F = -113k

FIG. 21 PRINCIPAL IN-PLANE STRESSES WING PLATES 1 AND 2 UNDER COMPRESSION

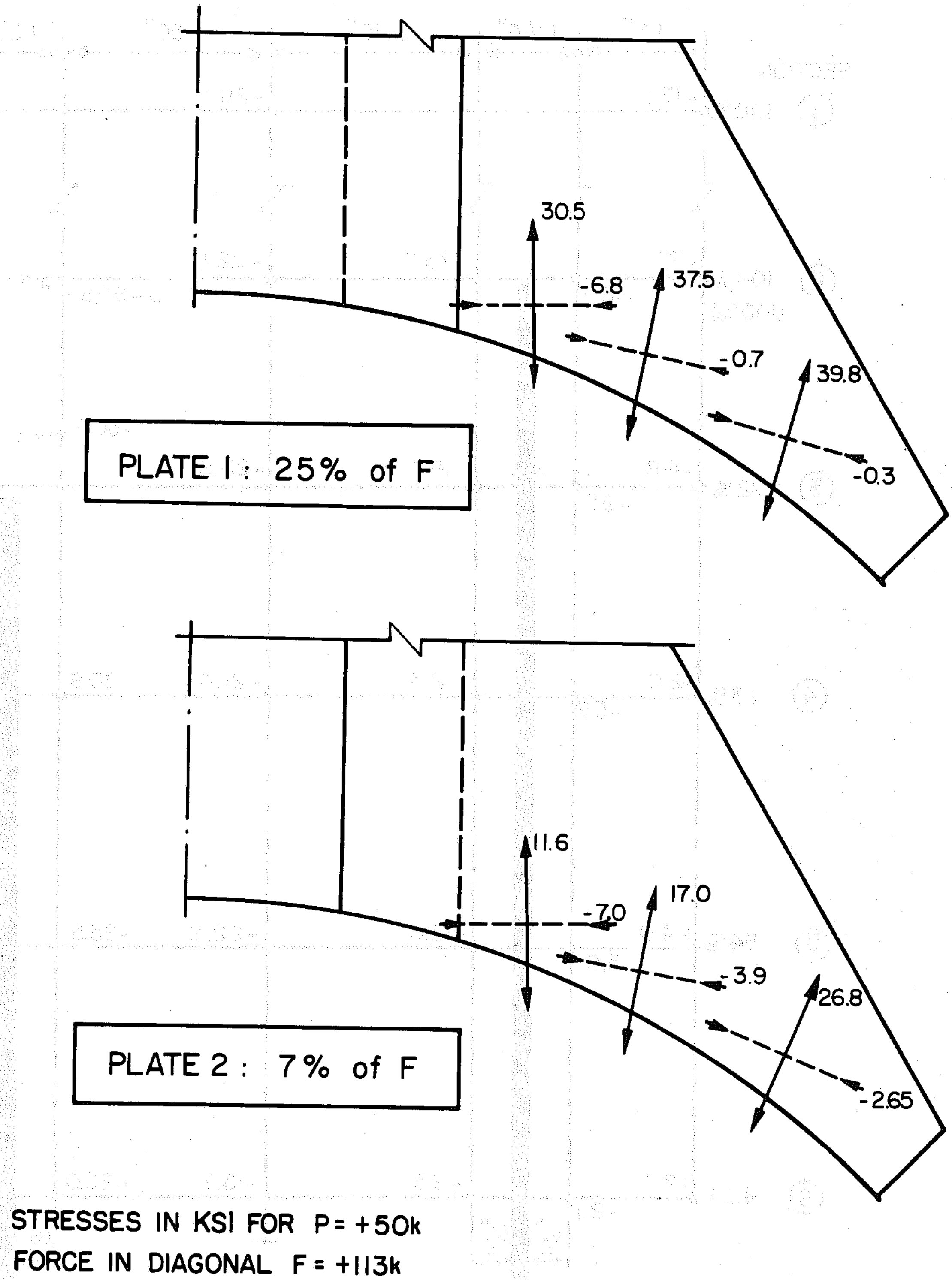

FIG. 22 PRINCIPAL IN-PLANE STRESSES WING PLATES 1 AND 2 UNDER TENSION

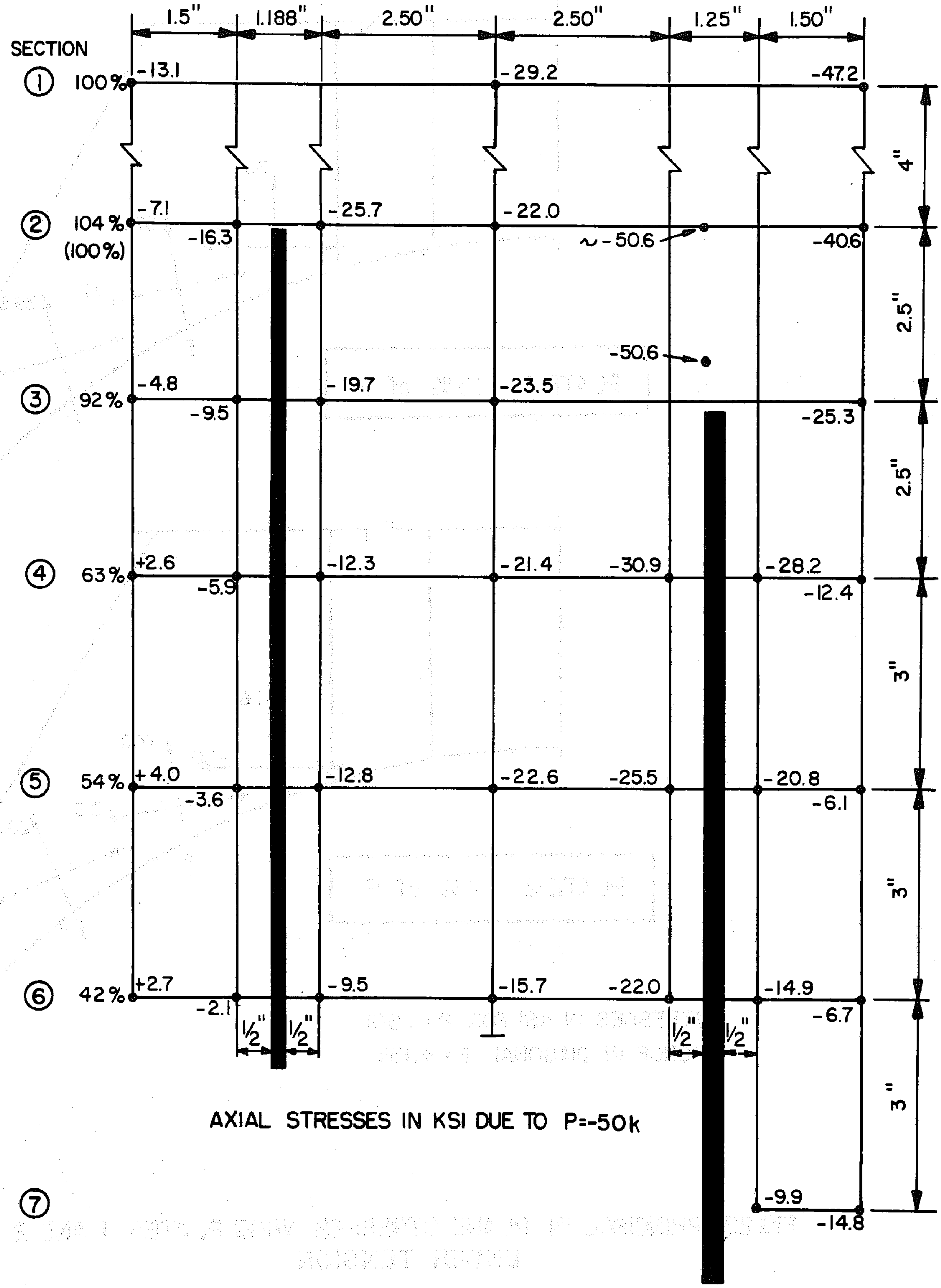

FIG. 23 DIAGONAL TUBE WALL STRESSES

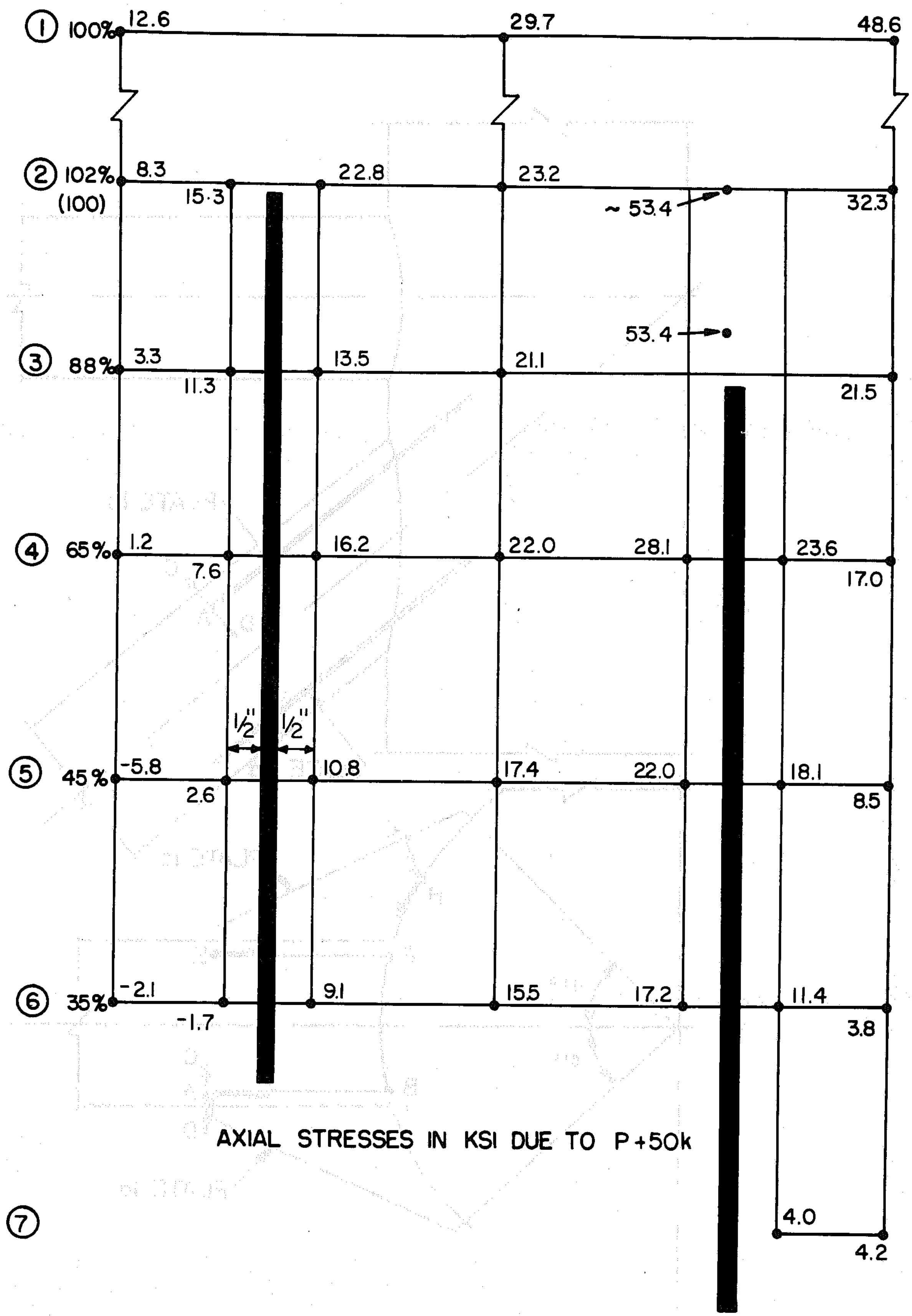

FIG. 24 DIAGONAL TUBE WALL STRESSES

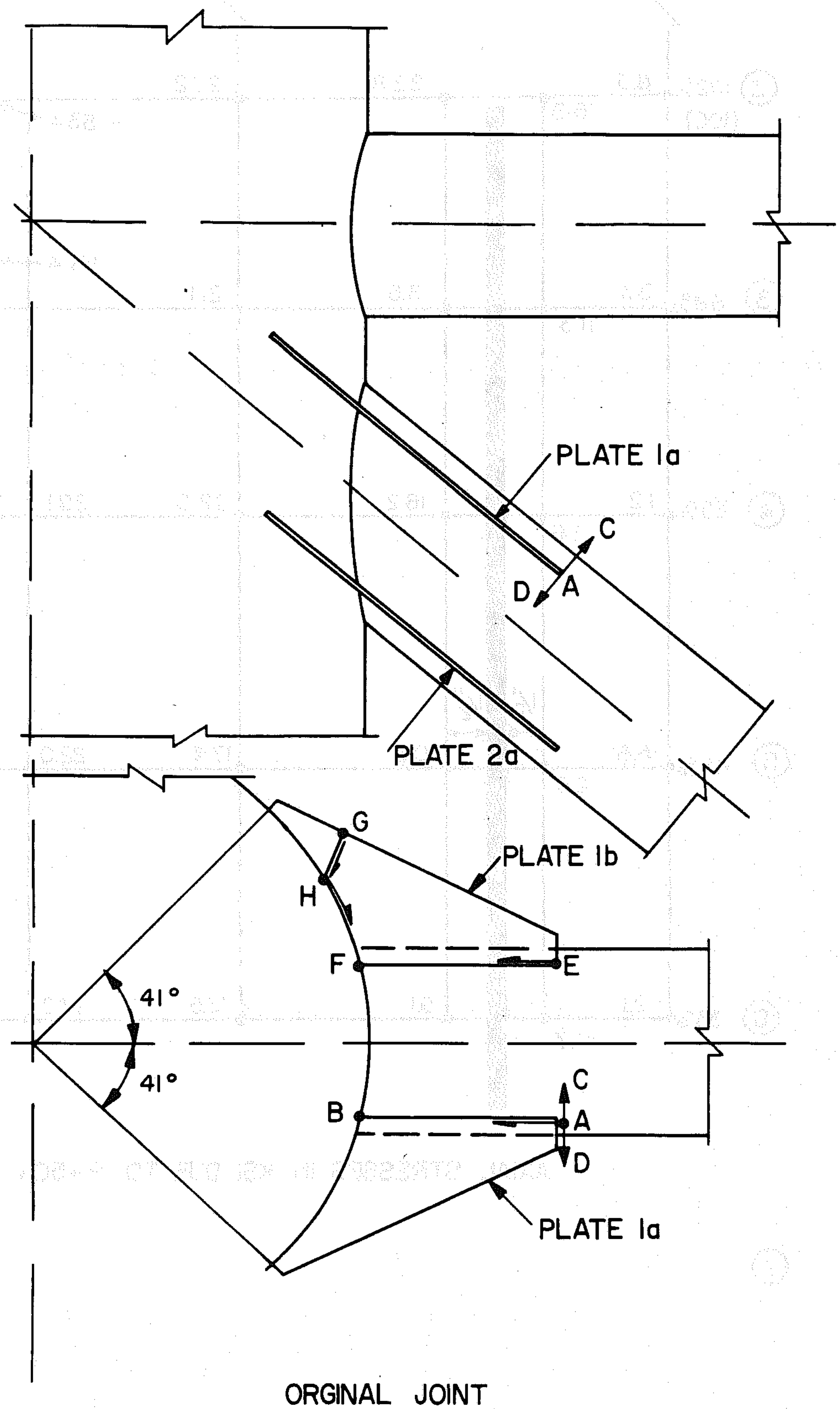

FIG. 25 CRACK PROPAGATION UNDER ALTERNATING LOAD

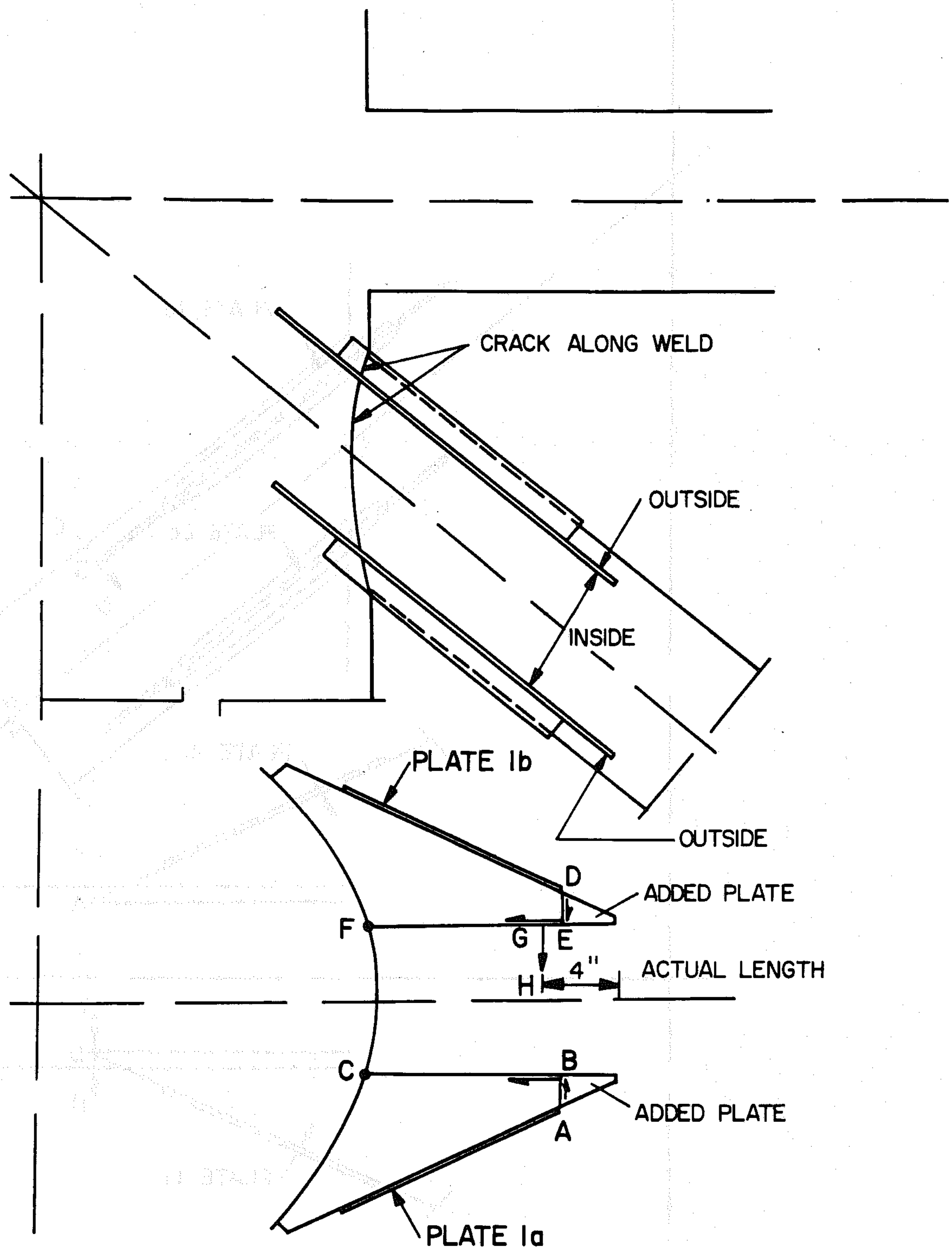

MODIFIED WING-PLATE JOINT

FIG. 26 CRACK PROPAGATION UNDER ALTERNATING LOAD

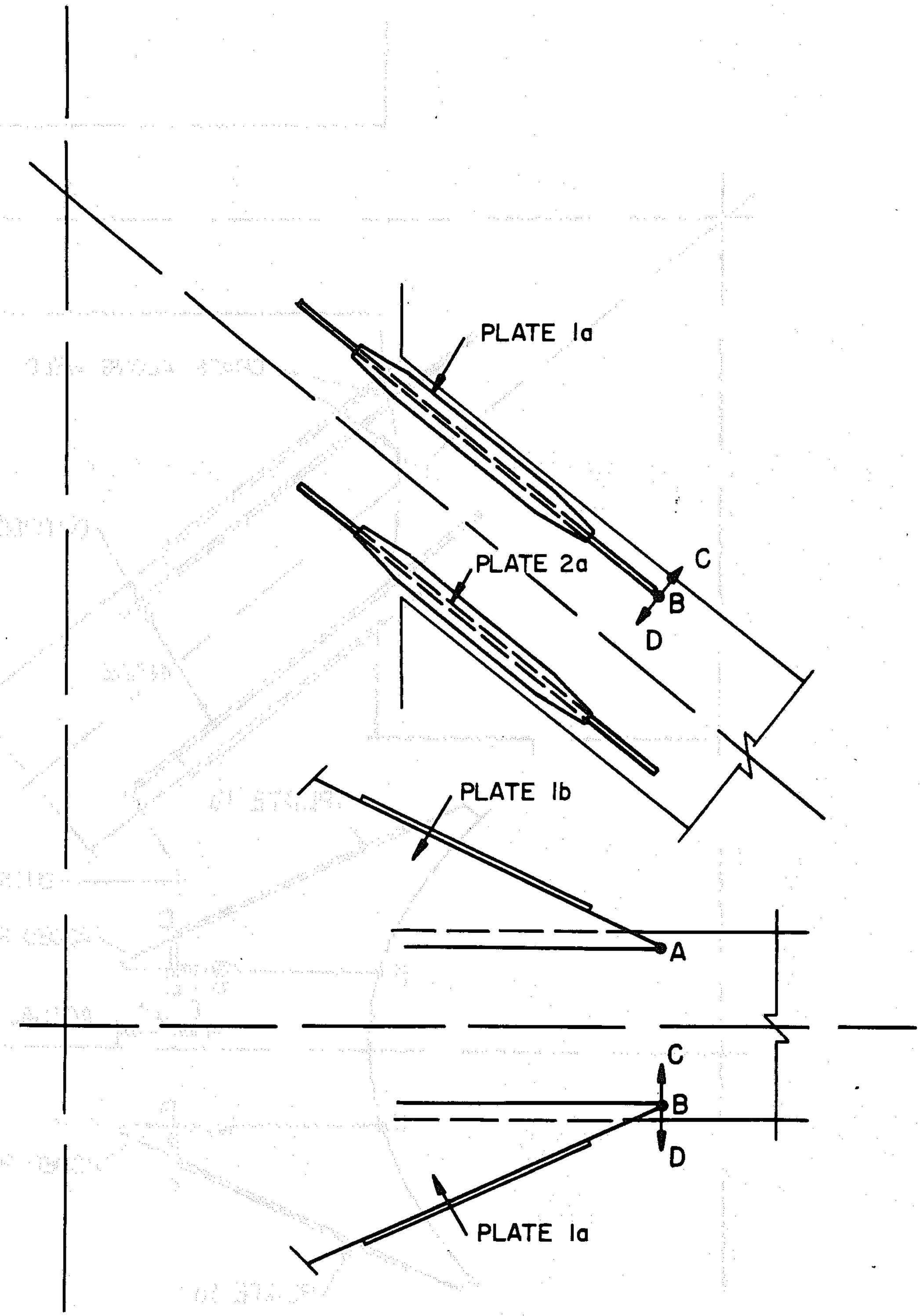

REVISED WING - PLATE JOINT

FIG. 27 CRACK PROPAGATION UNDER ALTERNATING LOAD